

Empirical Attenuation Equations for Vertical Ground Motion in Turkey

Erol Kalkan,^{a)} S.M.EERI, and Polat Gülkan,^{b)} M.EERI

In the aftermath of two destructive urban earthquakes in 1999 in Turkey, empirical models of strong motion attenuation relationships that have been previously developed for North American and European earthquakes have been utilized in a number of national seismic hazard studies. However, comparison of empirical evidence and estimates present significant differences. For that reason, a data set created from a suite of 100 vertical strong ground motion records from 47 national earthquakes that occurred between 1976 and 2002 has been used to develop attenuation relationships for strong ground motion in Turkey. A consistent set of empirical attenuation relationships was derived for predicting vertical peak and pseudo-absolute vertical acceleration spectral ordinates in terms of magnitude, source-to-site distance, and local geological conditions. The study manifests the strong dependence of vertical to horizontal (V/H) acceleration ratio on spectral periods and relatively weaker dependence on site geology, magnitude, and distance. The V/H ratio is found to be particularly significant at the higher frequency end of the spectrum, reaching values as high as 0.9 at short distances on soil sites. The largest long-period spectral ratios are observed to occur on rock sites where they can reach values in excess of 0.5. These results raise misgivings concerning the practice of assigning the V/H ratio a standard value of two-thirds. Hence, nonconservatism of this value at short periods and its conservatism at long periods underline the need for its revision, at least for practice in Turkey. [DOI: 10.1193/1.1774183]

INTRODUCTION

In 1999, Turkey was struck by two destructive earthquakes that occurred less than three months apart on the 1500-km-long North Anatolian Fault (NAF) that compares with the San Andreas Fault in California in terms of many of its features. The first of these two earthquakes hit the most densely populated urban environments, namely Kocaeli and Sakarya provinces, situated on an alluvial fan at the western part of the NAF with magnitude (M_W) 7.4. The second M_W 7.2 event destroyed the city (now provincial capital) of Düzce. These catastrophes were among the largest seismic events in the eastern Mediterranean basin during the last century and the first widely recorded and well studied NAF events. They provided the most extensive strong ground motion data set ever recorded in Turkey within about 170 km of the surface fault rupture, causing substantial structural damage, casualties, and economic loss. The first event (the 17 August

^{a)} University of California Davis, Department of Civil and Environmental Engineering, Davis, CA 95616

^{b)} Middle East Technical University, Department of Civil Engineering, Ankara, 06531 Turkey

1999, Kocaeli earthquake) generated 34 ground motion recordings associated with a 130 km surface rupture involving four distinct fault segments on the northernmost strand of the western extension of the NAF. The second event (the 12 November 1999, Düzce earthquake) triggered 20 instruments and caused 35 km of surface rupture on the eastern extension of the former event.

These two recent Turkish events were the latest among a successive westerly propagating earthquake sequence on the NAF that began with the magnitude 7.9 Erzincan earthquake in the eastern part of Turkey in 1939, and has generated ten destructive earthquakes having magnitudes greater than seven over past 60 years. This earthquake sequence similar to the toppling of domino pieces has now arrived at the gates of the most densely populated and the industrialized heart of Turkey, namely, the Istanbul metropolitan area (Parsons et al. 2000). The likelihood of experiencing devastating earthquakes on such a high-profile area in the near future has stimulated a number of studies toward national or regional seismic hazard and risk assessment studies for the country. One principal criticism for these concerns the blind implementation of empirical models of strong motion attenuation relations that have been previously proposed for North American and European earthquakes, despite the lack of proof for their cross applicability. The overprediction of these imported relationships to national earthquake data has been extensively questioned by a number of researchers (e.g., Gülkan and Kalkan 2002, Anderson et al. 2000, Rathje et al. 2000, Safak et al. 2000). There is evidence to serve as a reminder that there exists little support for the carefree import of attenuation relationships from other environments for use in important engineering applications elsewhere (Atkinson and Boore 1997, Gülkan and Kalkan 2002).

The assurance of earthquake-resistant design of structures and consequently minimization of losses from destructive earthquakes entail well-grounded ground motion prediction capability. With the increasing number of records now available in Turkey, it appears possible to explore the relationship between the general characteristics of spectral shapes derived from national strong ground motion records and list their parameters. This may help to overcome the lack of knowledge on the attenuation characteristics of Turkey, and inconsistencies in the implementation of foreign predictive equations. From this perspective, the development of attenuation relations for peak horizontal and spectral acceleration ordinates by Gülkan and Kalkan (2002) is an effort toward this goal. That attempt facilitated the construction of hazard-consistent site-specific design spectra for Turkey (Kalkan and Gülkan 2004a). To fill the gap in the mosaic, a consistent set of empirical attenuation relationships for predicting the vertical component of peak ground acceleration (PGA) and 5-percent-damped vertical spectral acceleration response spectra is now developed within the frame work of this study. The empirical predictive model for Turkey will be again presented in terms of moment magnitude, source-to-site distance, and local-site conditions with associated measures of uncertainty.

Since the characteristics of the ratio of vertical to horizontal strong ground motion were also sought, a separate set of empirical equations for predicting V/H spectral ratios was developed as a function of the same set of parameters used for the vertical attenuation model. Although it is possible to combine the two attenuation equations that individually predict the vertical and horizontal accelerations to obtain the spectral ratios, explicit determination of the correlation between the vertical and horizontal spectra

presents a unique opportunity to examine the validation of the proposed attenuation relationships. Therefore, characteristics of V/H spectral ratios were compared with those attained from both attenuation relationships and the actual ratios from recordings. This has further facilitated the investigation of the correctness of assigning spectral ratio a value of two-thirds in standard engineering practice in Turkey.

STRONG MOTION DATABASE

A data set from 100 vertical strong ground motion records from 47 earthquakes that occurred between 1976 and 2002 in Turkey has been created as the expanded and updated version of the previously compiled database on which the horizontal attenuation relationships were derived. The former data set consisted of 47 horizontal components of 19 earthquakes between 1976 and 1999, and in this new rendition several post-1999 events have been added. The current database includes data recorded within 250 km of the causative fault from earthquakes in the magnitude range of 4.5 to 7.4. All of the earthquakes occurred in the shallow crustal tectonic environment of Turkey. The list of these events and the number of recordings for each of their site categories are given in Table 1. A more comprehensive description of the strong motion database is presented in the Appendix, where station names and their abbreviations have been reproduced exactly as they were originally reported so that independent checks may be made. The epicenters of earthquakes and locations of the recording stations are marked on an active faulting map of Turkey, and exhibited in Figure 1. That figure is a reminder that the records used are mostly representative for the active tectonic environment of Turkey.

In the database, records were limited to the closer distances to minimize the complex propagation effects for longer distances. Earthquake size was characterized by moment magnitude M_w , as described by Hanks and Kanamori (1979). When original magnitudes were listed in other scales, conversion was done according to Wells and Copper-smith (1994) and Kramer (1996). The magnitudes were restricted to about $M_w \geq 4.5$ to emphasize those ground motions having greatest engineering interests, and to limit the analysis to the more reliably recorded events. Only one event, the 3 April 2002, M_w 4.2 Burdur earthquake, was not subjected to this limitation because of its high vertical acceleration (31 mg) recorded.

Several parameters in the former data set, including closest distance, magnitude, and site geology, were revised based on the collection of supplemental information after 1999. This revision was considered to be necessary since the data comes from a variety of sources of different accuracy and reliability. The sources of information are also referenced in the Appendix for each of their corresponding data points. Particularly, based on the broadcasted information by USGS, PEER, and COSMOS, some correction and fine-tuning were done on the distance and local-site condition parameters of the Kocaeli and Düzce events. Some of the station coordinates (e.g., Çerkeş Meteoroloji İst.) were corrected by ERD (Earthquake Research Department of General Directorate of Disaster Affairs) and thereby causing distance revision as large as 16.1 km in this new rendition.

For the source distance (r_{cl}), we adopted the closest horizontal distance (or Joyner and Boore distance) between the recording station and a point on the horizontal projection of the rupture zone on the earth's surface. However, for some of the smaller events,

Table 1. Earthquakes used in the analysis

Event No	Date (dd.mm.yy)	Event	Faulting Type *	Depth		Epicenter Coordinates *	Number of Recordings		
				M _w	(km) *		Rock	Soil	Soft Soil
1	19.08.1976	DENİZLİ	Normal	5.3	20.0	37.7100N - 29.0000E		1	
2	05.10.1977	ÇERKEŞ	Strike-Slip	5.4	10.0	41.0200N - 33.5700E			1
3	16.12.1977	İZMİR	Normal	5.5	24.0	38.4100N - 27.1900E			1
4	11.04.1979	MURADIYE	Strike-Slip	4.9	44.0	39.1200N - 43.9100E	1		
5	28.05.1979	BUCAK	Normal	5.8	111.0	36.4600N - 31.7200E	1		
6	18.07.1979	DURSUNBEY	Strike-Slip	5.3	7.0	39.6600N - 28.6500E	1		
7	30.06.1981	HATAY	Strike-Slip	4.7	63.0	36.1700N - 35.8900E		1	
8	05.07.1983	BİGA	Reverse	6.1	7.0	40.3300N - 27.2100E	2		1
9	30.10.1983	HORASAN-NARMAN	Strike-Slip	6.5	16.0	40.3500N - 42.1800E			2
10	29.03.1984	BALIKESİR	Strike-Slip	4.5	0.0	39.6400N - 27.8700E			1
11	17.06.1984	FOÇA	Normal	5.0	0.0	38.8700N - 25.6800E	1		
12	12.08.1985	KIĞI	Strike-Slip	4.9	29.0	39.9500N - 39.7700E		1	
13	06.12.1985	KÖYCEĞİZ	Strike-Slip	4.6	0.0	36.9700N - 28.8500E			1
14	05.05.1986	MALATYA	Strike-Slip	6.0	4.0	38.0200N - 37.7900E	1		
15	06.06.1986	SÜRGÜ (MALATYA)	Strike-Slip	6.0	11.0	38.0100N - 37.9100E	1	1	
16	20.04.1988	MURADIYE	Strike-Slip	5.0	55.0	39.1100N - 44.1200E	1		
17	12.02.1991	İSTANBUL	Strike-Slip	4.8	10.0	40.8000N - 28.8200E	1		
18	13.03.1992	ERZİNCAN	Strike-Slip	6.9	27.0	39.7200N - 39.6300E		1	1
19	06.11.1992	SIVRİHİSAR	Normal	6.1	17.0	38.1600N - 26.9900E			1
20	03.01.1994	İSLAHİYE	Strike-Slip	5.0	26.0	37.0000N - 35.8400E		1	
21	24.05.1994	GİRİT	Normal	5.0	17.0	38.6600N - 26.5400E	1		
22	13.11.1994	KÖYCEĞİZ	Strike-Slip	5.2	10.0	36.9700N - 28.8090E			1
23	29.01.1995	TERCAN	Strike-Slip	4.8	31.0	39.9008N - 40.9900E		1	
24	26.02.1995	VAN	Strike-Slip	4.7	N/A	38.6000N - 43.3300E			1
25	01.10.1995	DİNAR	Normal	6.4	5.0	38.1100N - 30.0500E		1	1
26	02.04.1996	KUŞADASI	Normal	4.9	33.0	37.7800N - 26.6400E			1
27	14.08.1996	MERZİFON	Strike-Slip	5.4	10.0	40.7900N - 35.2300E			1
28	21.01.1997	BULDAN	Normal	4.8	9.0	38.1200N - 28.9200E		1	
29	22.01.1997	HATAY	Strike-Slip	5.5	23.0	36.1400N - 36.1200E		2	
30	28.02.1997	MERZİFON	Strike-Slip	4.7	5.0	40.6800N - 35.3000E			1
31	03.11.1997	MALAZGİRT	Strike-Slip	4.9	N/A	38.7600N - 42.4000E			1
32	04.04.1998	DİNAR	Normal	4.6	7.0	38.1400N - 30.0400E		1	1
33	27.06.1998	ADANA-CEYHAN	Strike-Slip	6.3	18.0	36.8500N - 35.5500E	1	3	2
34	09.07.1998	BORNOVA	Normal	5.1	21.0	38.0800N - 26.6800E			1
35	17.08.1999	KOCAELİ	Strike-Slip	7.4	18.0	40.7000N - 29.9100E	9	6	11
36	11.11.1999	SAPANCA-ADAPAZARI	Strike-Slip	5.7	8.9	40.8100N - 30.2000E	1		
37	12.11.1999	DÜZCE	Strike-Slip	7.2	10.0	40.7400N - 31.2100E	4	1	7
38	06.06.2000	ÇANKIRI-ORTA	Strike-Slip	6.1	10.0	40.7200N - 32.8700E			1
39	23.08.2000	HENDEK-AKYAZI	Strike-Slip	5.1	15.3	40.6800N - 30.7100E	1		3
40	04.10.2000	DENİZLİ	Normal	4.7	8.4	37.9100N - 29.0400E		1	
41	15.11.2000	TATVAN-VAN	Strike-Slip	5.5	10.0	36.9300N - 44.5100E			1
42	10.07.2001	ERZURUM-PASINLER	Strike-Slip	5.4	5.0	39.8273N - 41.6200E			1
43	26.08.2001	YIĞILCA-DÜZCE	Strike-Slip	5.4	7.8	40.9455N - 31.5728E			1
44	02.12.2001	VAN	Strike-Slip	4.5	5.0	38.6170N - 43.2940E			1
45	03.02.2002	SULTANDAĞI-ÇAY	Reverse	6.5	5.0	38.5733N - 31.2715E		1	1
46	03.04.2002	BURDUR	Strike-Slip	4.2	5.0	37.8128N - 30.2572E		1	
47	14.12.2002	ANDIRIN-K. MARAŞ	Strike-Slip	4.8	13.6	37.4720N - 36.2210E		1	
Total							27	26	47

* Data source: Earthquake Research Department (ERD), General Directorate of Disaster Affairs

N/A: Hypocentral depth information is not available

rupture surfaces have not been defined clearly, so epicentral distances have been used instead. We believe that use of epicentral distance does not introduce significant bias because the dimensions of the rupture area for small earthquakes are usually much smaller than the distance to the recording stations. The distribution of the earthquakes in this new data set in terms of magnitude, site geology, and source distance is demonstrated in Figure 2, and our entire ensemble with respect to vertical PGA values and closest hori-

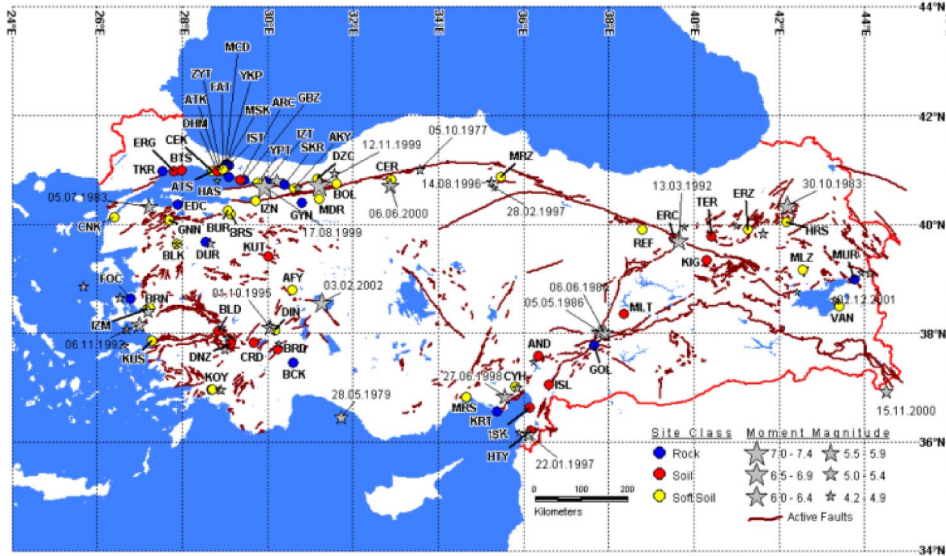


Figure 1. Epicenters of earthquakes and locations of strong motion recording stations on active faulting map of Turkey.

zontal distance is exhibited in Figure 3. The paucity of data from the small number of normal-faulting (14 recordings) and reverse-faulting earthquakes (5 recordings) in the data set did not permit us to treat the faulting mechanism as a parameter, as this would

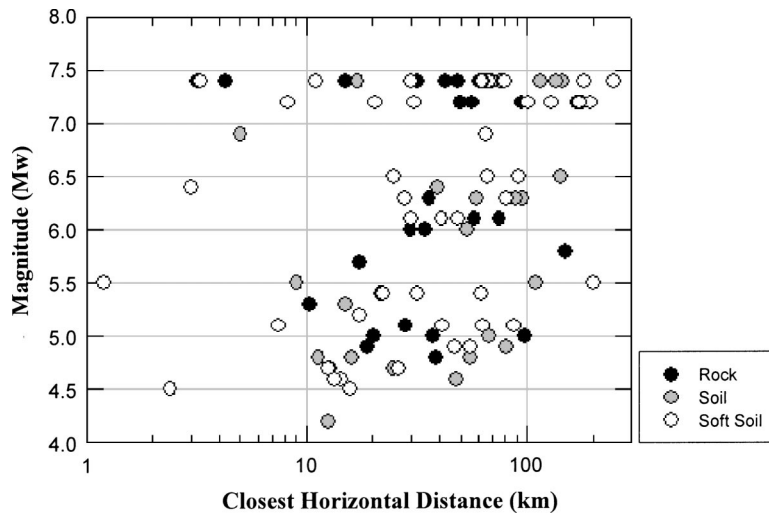


Figure 2. Distribution of records in the database with respect to magnitude and closest horizontal distance for rock, soil, and soft-soil site conditions.

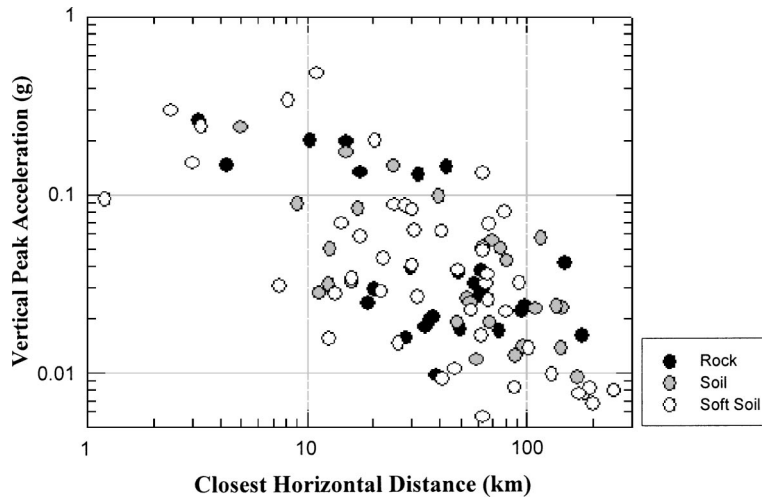


Figure 3. Distribution of records in the database with respect to vertical PGA and closest horizontal distance for rock, soil, and soft-soil site conditions.

give undue weight to particular faulting categories. Therefore, normal, reverse, and strike-slip earthquakes were combined into a single faulting category. Until additional data becomes available, this will constitute a constraint for the presented results in this paper.

The data used in the analysis represents main shocks recorded mostly in small or medium-sized state-owned buildings up to three stories tall because the strong motion stations in Turkey are collocated with institutional facilities for ease of access, phone hook-up, and security. This proximity contaminates the seismograms and causes modified acceleration records (e.g., Anderson et al. 2001). This is one of the unavoidable causes of epistemic parametric uncertainties in our study, but there are other attributes that must be mentioned. The first is our omission of aftershock data. Most of these come from the two major 1999 events, and contain free-field data that we did not wish to commingle with the rest of the data. We also eliminated the few records for which the peak acceleration caused by the main shock is less than about 10 mg despite their magnitudes above the threshold of (M_w) 4.5. Such a limitation in the data set resulted in exclusion of aftershock data recorded in the permanent stations as well.

When we consider the effects of geological conditions on ground motion and response spectra, the widely accepted method of reflecting these effects is to classify the recording stations according to the shear-wave velocity profiles of their substrata in the upper 30 m, Boore et al. (1993, 1997). Unfortunately, shear-wave velocity and detailed site description are incomplete for most stations in Turkey. It is nonetheless possible to classify the 65 permanent strong motion stations in our data set into three categories roughly by analogy with information in geology of their locations. The type of geologic material underlying each recording station was obtained in a number of ways: consultation with geologists at ERD, various geologic maps, past earthquake reports, and geo-

logical references prepared for Turkey. Based on this collected qualitative data, we prefer to use more general classification of site geology that could be applied uniformly and would be broadly applicable. Therefore, we divided soil groups for recording stations in Turkey into three categories: rock (with average shear wave velocity, V_S , over 30m depth is 700 m/sec); soil (V_S is 400 m/sec); and soft soil (V_S is 200 m/sec). The correspondence between these values and more widely accepted soil categories is obviously tenuous.

VERTICAL ATTENUATION RELATIONSHIPS

Attenuation relationships used in this study were developed from the general form of the equation proposed by Spudich et al. (1999). Originally, their equation was developed to estimate the horizontal PGA and 5-percent-damped peak spectral velocity (PSV). With modifications on this equation, we obtained the ground motion estimation equation for vertical component of PGA and 5-percent-damped pseudo-absolute vertical spectral accelerations. The general form of this regression relation is of the form

$$\ln Y_V = C_1 + C_2(M-6) + C_3(M-6)^2 + C_4(M-6)^3 + C_5 \ln r + C_6\Gamma_1 + C_7\Gamma_2 + P\sigma \quad (1)$$

$$r = (r_{cl}^2 + h^2)^{1/2} \quad (2)$$

where Y_V is the vertical ground motion parameter (vertical PGA or pseudo-absolute vertical spectral acceleration in g), M is the moment magnitude, r_{cl} is the closest horizontal distance (or Joyner-Boore distance) from the station to a site of interest in km, and C_1 , C_2 , C_3 , C_4 , C_5 , and h are the regression parameters to be determined. C_6 and C_7 are soil and soft-soil amplification parameters with respect to rock. In this equation, h is a fictitious depth, and Γ is an index variable controlling the local geological conditions. For rock sites $\Gamma_1 = \Gamma_2 = 0$; for soil sites $\Gamma_1 = 1$ and $\Gamma_2 = 0$; for soft soil sites $\Gamma_1 = 0$ and $\Gamma_2 = 1$. The additional cubical term for magnitude was introduced in Equation 1 to compensate for the controversial effects of sparsity of the Turkish earthquakes, and consequently resulted in a better fit to the actual data. In this equation, distance term shows the geometrical attenuation, whereas the terms of magnitude and site conditions represent anelastic attenuation. The standard deviation of $\ln Y_V$ is σ , and the P takes a value of 0 for mean values and 1 for 84-percentile of $\ln Y_V$.

Considerable exploratory analyses for obtaining simultaneously the best estimates and least standard error justified the use of two-stage multivariate nonlinear regression analysis for determining the coefficients in the median attenuation equation via decoupling the site effects from magnitude and distance dependence. Thus the entire data was regressed in the first stage disregarding the local-site effects, yielding the parameters C_1 to C_5 and h . In this stage, magnitude and distance are the only independent parameters. Local-site effects were determined in the next stage, thereby constraining the initially estimated parameters (C_1 to C_5 and h). Thereafter, the rock data was first regressed to update the value of offset factor C_1 using a transferring parameter C_8 . Then the soil amplification factors, C_6 and C_7 , were derived by performing separate regression analyses on soil and soft soil data constraining the aforementioned parameters and using updated C_1 (i.e., $C_{1\text{updated}} = C_1 + C_8$). This exercise was performed on vertical PGA and the pseudo-absolute acceleration spectral ordinates individually. The spectral ordinates at

5 percent of critical damping were kept in the range of 0.1 to 2.0 sec (a total of 46 periods) at the same intervals used in the Caltech volumes (1972). The coefficients for estimating the vertical component of pseudo-absolute acceleration response by Equation 1 are listed in Table 2. The resulting parameters can be used to produce attenuation relationships that predict the vertical response spectra over the full range of magnitudes (M_w 4.5 to 7.4) and distances (r_{cl}) up to 200 km. The resultant attenuation curves for vertical PGA for rock, soil, and soft soil sites are shown in Figure 4 for magnitude 7.0 and 5.0 earthquakes. The complete vertical spectra constructed based on Equation 1 and Table 2 of coefficients is presented in Figure 5 for M_w 6.0 and 7.4 earthquakes at a distance of 10 km. Also shown are the horizontal spectra from our earlier work for comparison (Gülkan and Kalkan 2002). At long periods, the differences between soft soil and rock sites are barely distinguishable in vertical spectra, whereas in horizontal spectra these differences are more noticeable. There also exists a clear picture of increase in the predominant period with increase in magnitude in horizontal spectra; however, such a trend is less significant in the vertical spectra. It should be also noted that the predominant periods of the horizontal spectra (0.2 to 0.5 sec) are longer than those of the vertical spectra (around 0.1 sec).

The regression results were used to compute the estimation error for both vertical component of PGA and spectral accelerations at individual periods. The standard deviation of the residuals ($\ln\sigma$), expressing the random variability of ground motions, is in the range of 0.5 to 0.7 for rock and soil sites and 0.4 to 0.9 for soft soil sites. Residuals plots of vertical PGA estimation based on Equation 1 for the full data set as functions of magnitude and closest distance are presented in Figures 6 and 7 together with their linear best-fit relations. With respect to magnitude term, no significant trends are observed either for the full data set (Figure 6a) or for any of the site categories (Figure 6b). This may serve as evidence for magnitude independency of the residuals. However, the perspective is slightly different for the distance parameter, although no significant trends exist for the full data set (Figure 7a), the minor trends are noticed in Figure 7b particularly for the soil and soft soil data. This figure shows that distance dependence is affected by a few high residuals at longer distances, namely for more than 100 km. Consequently, we believe that the distance dependence of residuals in Figure 7b is in part caused by the sparseness of the rock and soft soil data at farther distances (Figure 2) in our database.

COMPARISON WITH RECENT ATTENUATION EQUATIONS

Since there are no published vertical attenuation relationships in the literature for Turkey, the attenuation relations given in Equation 1 with the coefficients in Table 2 could only be compared with those recently developed by Ambraseys et al. (1996) and Campbell (1997). Ambraseys et al. (1996) proposed their empirical equations for the estimation of vertical response spectra for Europe, but they have also investigated the near-field V/H spectral ratios using worldwide earthquakes. In their vertical spectra, local soil effects were considered in three categories as rock ($V_s > 750$ m/sec), stiff soil (360 m/sec $< V_s < 750$ m/sec), and soft soil ($V_s < 360$ m/sec). Campbell (1997) studied

Table 2. Coefficients for Equation 1, for vertical PGA and 5-percent-damped spectral accelerations

$\ln(Y_v) = C_1 + C_2(M - 6) + C_3(M - 6)^2 + C_4(M - 6)^3 + C_5 \ln r + C_6 \Gamma_1 + C_7 \Gamma_2 + P \sigma$ with $r = (r_{cr}^2 + h^2)^{1/2}$												
Period (sec)	C_1	C_2	C_3	C_4	C_5	C_6	C_7	h	nrec*	σ_{Rock}	σ_{Soil}	$\sigma_{S, Soil}$
PGA **	0.055	0.387	-0.006	0.041	-0.944	0.277	0.030	7.72	100	0.629	0.607	0.575
0.100	2.009	0.483	-0.042	-0.007	-1.250	0.163	0.006	14.69	95	0.672	0.713	0.598
0.110	1.832	0.601	-0.020	-0.085	-1.206	0.160	0.057	14.29	96	0.684	0.692	0.609
0.120	1.684	0.664	0.014	-0.131	-1.175	0.154	0.030	10.89	97	0.653	0.695	0.589
0.130	1.732	0.641	-0.023	-0.097	-1.176	0.201	0.008	12.84	97	0.595	0.692	0.548
0.140	1.753	0.553	-0.017	-0.053	-1.177	0.241	-0.001	13.95	98	0.586	0.754	0.568
0.150	1.231	0.489	-0.024	-0.020	-1.050	0.191	-0.053	8.93	99	0.609	0.756	0.583
0.160	1.120	0.512	-0.024	-0.025	-1.024	0.216	-0.063	7.99	100	0.604	0.735	0.567
0.170	1.110	0.472	-0.043	0.026	-1.058	0.133	-0.035	9.49	97	0.592	0.602	0.542
0.180	1.294	0.439	-0.054	0.050	-1.055	0.112	-0.068	10.42	96	0.572	0.602	0.486
0.190	1.202	0.453	-0.040	0.058	-1.053	0.116	0.019	11.10	99	0.582	0.661	0.540
0.200	0.967	0.484	0.005	0.032	-1.013	0.191	0.023	12.42	97	0.592	0.678	0.515
0.220	0.857	0.551	-0.020	0.000	-0.997	0.156	0.052	12.44	96	0.620	0.582	0.465
0.240	0.509	0.424	-0.027	0.077	-0.919	0.263	0.070	11.60	98	0.629	0.681	0.508
0.260	0.301	0.386	-0.041	0.109	-0.868	0.261	0.011	9.40	98	0.653	0.681	0.481
0.280	0.043	0.388	-0.049	0.103	-0.808	0.252	0.031	10.08	97	0.620	0.570	0.520
0.300	0.451	0.422	-0.088	0.119	-0.903	0.230	0.101	13.43	99	0.645	0.654	0.580
0.320	-0.046	0.420	-0.097	0.127	-0.803	0.360	0.151	11.36	97	0.607	0.602	0.604
0.340	-0.158	0.465	-0.115	0.122	-0.781	0.379	0.164	10.81	98	0.620	0.592	0.611
0.360	-0.264	0.491	-0.155	0.125	-0.753	0.359	0.136	8.96	99	0.615	0.588	0.604
0.380	-0.481	0.433	-0.189	0.150	-0.706	0.389	0.135	7.49	98	0.576	0.566	0.582
0.400	-0.634	0.347	-0.184	0.197	-0.676	0.421	0.087	7.40	98	0.599	0.555	0.552
0.420	-0.836	0.361	-0.182	0.192	-0.628	0.428	0.072	6.77	98	0.622	0.544	0.554
0.440	-1.002	0.424	-0.182	0.160	-0.593	0.423	0.100	6.33	98	0.628	0.514	0.556
0.460	-1.190	0.461	-0.183	0.137	-0.561	0.439	0.150	5.43	98	0.655	0.509	0.571
0.480	-1.340	0.494	-0.188	0.116	-0.536	0.456	0.190	4.70	98	0.674	0.540	0.597
0.500	-1.444	0.517	-0.191	0.095	-0.522	0.422	0.235	4.33	96	0.777	0.540	0.626
0.550	-1.256	0.545	-0.207	0.099	-0.562	0.426	0.129	5.65	98	0.692	0.555	0.611
0.600	-1.370	0.548	-0.234	0.120	-0.544	0.424	0.097	5.40	97	0.696	0.554	0.588
0.650	-1.423	0.573	-0.227	0.121	-0.551	0.352	0.150	5.38	97	0.693	0.607	0.696
0.700	-1.341	0.695	-0.194	0.071	-0.595	0.225	0.150	5.47	98	0.682	0.516	0.693
0.750	-1.419	0.724	-0.202	0.073	-0.594	0.188	0.177	5.32	98	0.679	0.522	0.696
0.800	-1.519	0.713	-0.145	0.061	-0.593	0.265	0.196	6.73	98	0.696	0.632	0.735
0.850	-1.578	0.761	-0.160	0.036	-0.588	0.312	0.231	6.73	97	0.689	0.572	0.764
0.900	-1.662	0.742	-0.161	0.053	-0.588	0.314	0.228	6.60	97	0.683	0.533	0.800
0.950	-1.723	0.727	-0.152	0.076	-0.584	0.288	0.171	5.49	97	0.687	0.502	0.839
1.000	-1.712	0.752	-0.137	0.079	-0.593	0.206	0.052	4.16	97	0.721	0.498	0.812
1.100	-1.731	0.837	-0.214	0.072	-0.581	0.173	0.041	4.08	97	0.721	0.525	0.897
1.200	-1.816	0.833	-0.256	0.097	-0.579	0.233	0.062	4.48	97	0.645	0.532	0.867
1.300	-1.814	0.910	-0.284	0.080	-0.602	0.256	0.089	4.61	97	0.677	0.610	0.849
1.400	-1.903	0.928	-0.309	0.072	-0.585	0.231	0.048	4.64	98	0.681	0.681	0.803
1.500	-1.932	0.974	-0.279	0.025	-0.597	0.160	0.032	4.94	99	0.675	0.693	0.872
1.600	-2.068	0.965	-0.288	0.038	-0.583	0.178	0.027	4.43	99	0.678	0.690	0.891
1.700	-2.150	1.023	-0.311	0.021	-0.581	0.230	0.030	3.62	99	0.705	0.710	0.904
1.800	-2.321	1.010	-0.310	0.034	-0.559	0.273	0.034	3.74	98	0.735	0.743	0.892
1.900	-2.348	1.048	-0.323	0.016	-0.570	0.301	0.064	4.26	97	0.738	0.767	0.911
2.000	-2.330	1.111	-0.337	-0.009	-0.593	0.280	0.104	3.09	98	0.729	0.740	0.906

* Number of records used for two-staged nonlinear regression

** Vertical component of peak ground acceleration

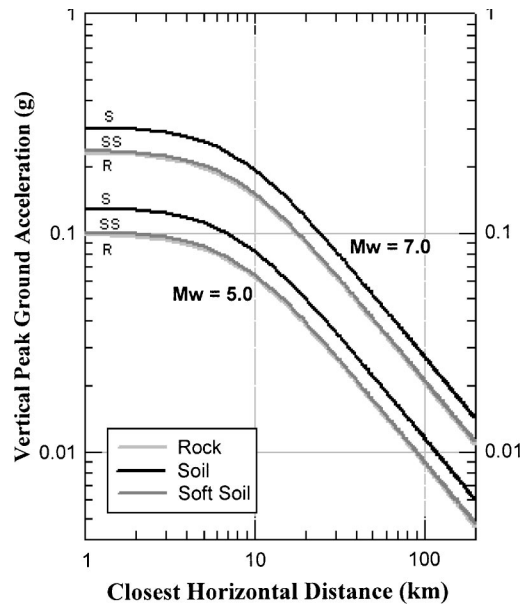


Figure 4. Curves of vertical PGA versus distance for magnitude (M_w) 5.0 and 7.0 earthquakes at rock (R), soil (S), and soft-soil (SS) site conditions.

the attenuation characteristics of vertical ground motion using worldwide earthquakes in a global manner, and his equations pertain to alluvium (or firm soil), soft rock, and hard rock site conditions.

Figure 8 gives the comparison of our model with that of Ambraseys et al. (1996) for soft-soil site conditions. The three-dimensional attenuation surfaces shown in this figure give more insight into the picture by setting the magnitude term free of constraint. This figure exhibits faster attenuation of Ambraseys's model along both magnitude and distance axes at close distances in contrast to our long distance predictions. The attenuation of vertical PGA for a magnitude 7.4 earthquake for three subsoil conditions is next compared with those recent models in Figure 9. The measured data points from the 1999 Kocaeli event are also marked to show how the prediction curves fit the observations. The best estimate curves in these figures correspond to mean values. Also drawn are the plus and minus sigma curves of our model to show the prediction band corresponding to 84 percentile probability. The peak acceleration estimation given herein possesses a standard deviation ($\ln\sigma$) of 0.629, 0.607, and 0.575 for rock, soil, and soft soil sites, respectively. Comparing the predictions of different models, we observe that our ground motion predictions at short distances are lower than the others. However, at farther distances this effect is counterbalanced, resulting in higher predictions. Notably, there exists a significant similarity in our attenuation curves and those of Ambraseys', particularly after 10 km of source-to-site distance. It is also noteworthy that comparison of predicted horizontal spectra from our earlier work with those attained from other horizontal attenuation models exhibited similar trends.

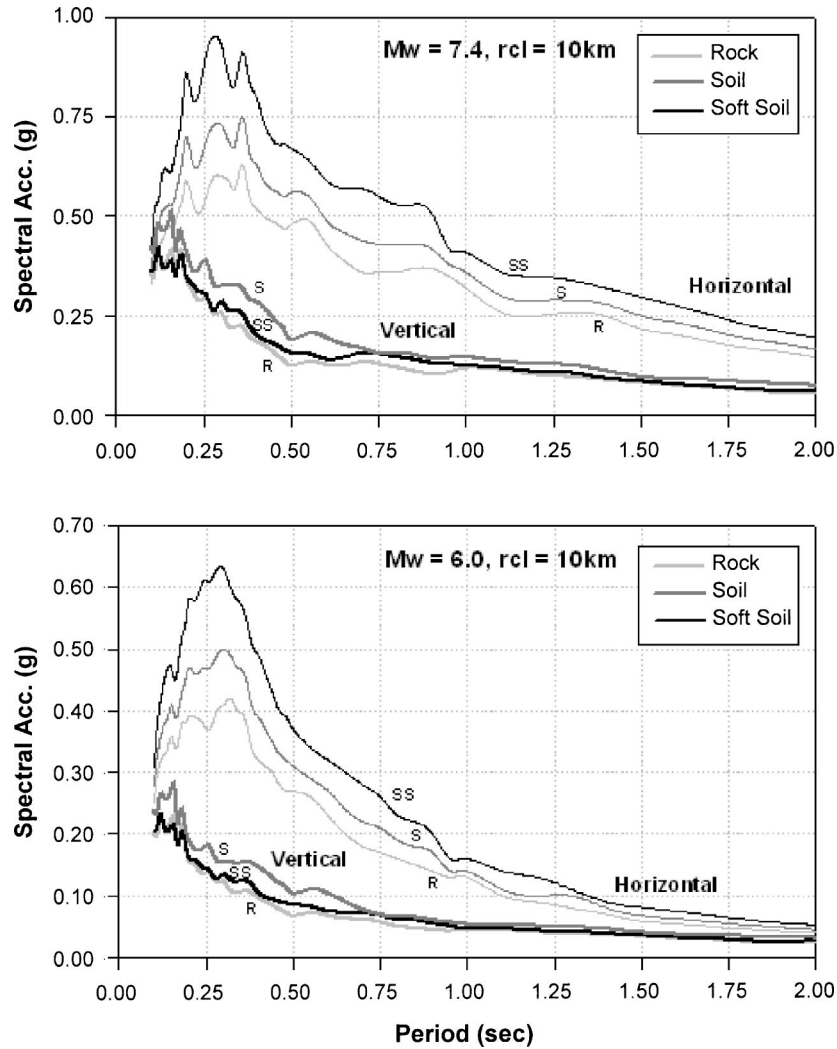


Figure 5. Expected mean vertical spectra for rock (R), soil (S), and soft-soil (SS) site classes, for (M_w) 7.4 and 6.0 earthquakes at a closest horizontal distance of 10 km and comparison of horizontal spectra of Gülkan and Kalkan (2002).

We have next compared the recorded spectra for several strong motions records of the Erzincan (1992), Dinar (1995), Kocaeli (1999), and Düzce (1999) earthquakes with our predicted vertical spectra based on Equation 1 with the coefficients in Table 2. These comparisons are presented in Figure 10. With the exception of the Mudurnu record of the Düzce earthquake (MDR at $r_{cl}=30.9$ km), the others were intentionally selected near-field records ($r_{cl}<15$ km) to emphasize the ground motions of particular engineer-

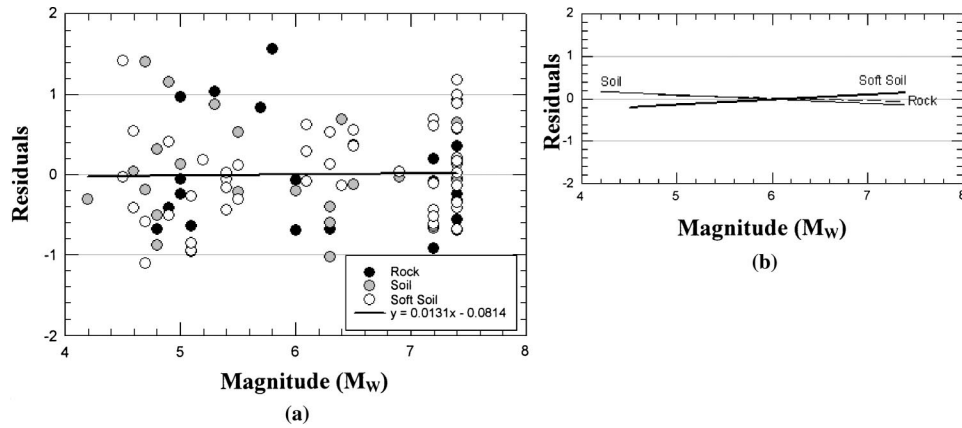


Figure 6. (a) Residuals of natural logarithm of vertical PGA from Equation 1 with Table 2 coefficients as a function of magnitude for three different site categories; (b) Regressions of residuals of natural logarithm of vertical PGA on distance for three different site categories.

ing significance. The comparisons in this figure reveal that estimated response curves are in general agreement with the computed responses of recorded accelerations at various magnitude, distance, and site categories.

PREDICTION OF V/H SPECTRAL RATIO

Although the current building codes and seismic provisions stimulated the use of two-thirds of horizontal acceleration as the vertical component of design acceleration (as

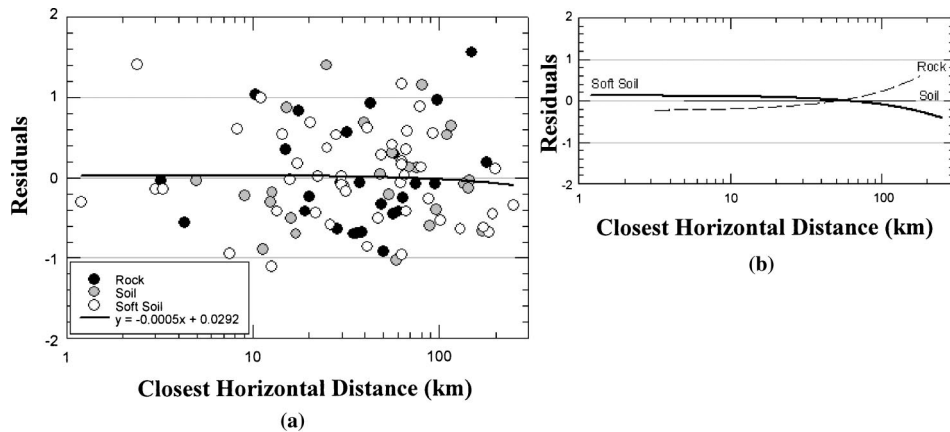


Figure 7. (a) Residuals of natural logarithm of vertical PGA from Equation 1 with Table 2 coefficients as a function of closest horizontal distance for three different site categories; (b) Regressions of residuals of natural logarithm of vertical PGA on magnitude for three different site categories.

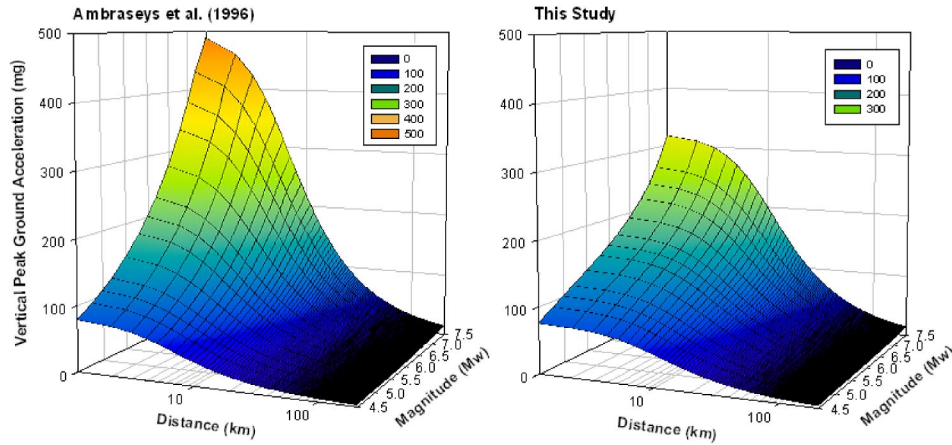


Figure 8. Comparison of our predictive model for vertical PGA with that of Ambraseys et al. (1996) on a 3-D plot for magnitude range of 4.5 to 7.5 and distance range of 0 to 200 km.

first proposed by Newmark and Hall in 1982), its accuracy is subject to misgivings particularly for the regions exposed to high seismicity. In fact, the V/H spectral ratio has been recently observed to be greater than two-thirds near the source of moderate to large earthquakes and less than this threshold at larger distances (Campbell 1985, Abrahamson and Litehiser 1989). It is therefore a necessity to obtain a clear understanding of variations between vertical and horizontal components of ground motion for reliable seismic hazard and risk assessment studies. For that purpose, a consistent set of equations for predicting the V/H spectral ratios, R , for Turkey was developed utilizing the same data set given in Appendix. Principally, it is also possible to determine R by predicting vertical and horizontal accelerations separately (by means of predeveloped attenuation relationships). However, we preferred to perform a regression directly on spectral ratios, and left the second procedure for the cross-check of our results. Therefore, 100 time histories populated for the derivation of vertical attenuation relationships were redistilled to obtain the envelope of the ratio of two horizontal spectra to vertical spectra for each recording.

Two-stage linear regression was next performed considering various combinations of predictive formulas. The equation presented below as Equation 3 was recommended at the end to predict the V/H spectral ratios (for 5 percent of critical damping) at each spectral period. The attenuation model applied for that purpose is linear in terms of moment magnitude and closest distance, and is close to the form of the equation given by Ambraseys et al. (1996). Their empirical equation was developed to predict the spectral ratios of near-field earthquakes using both the worldwide and European data sets separately and without treating the local-site conditions as a parameter. However, the analysis results here appraise the clear distinction between different site conditions in terms of spectral ratios at each response period, thereby suggesting the implementation of these effects into the empirical model. Based on this premise, two additional parameters were

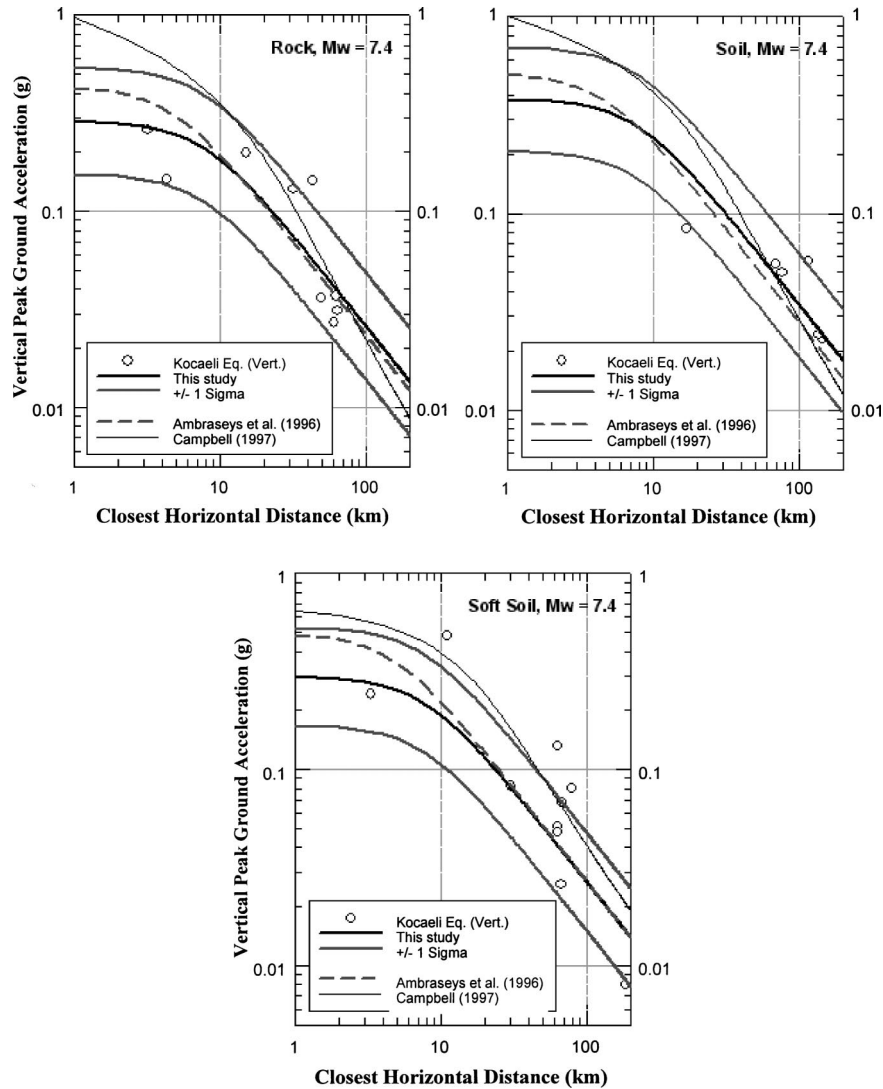


Figure 9. Curves for vertical PGA versus distance for magnitude 7.4 earthquake at rock, soil, and soft-soil site conditions.

incorporated into the equation of Ambraseys et al. (1996) to reflect the influence of local-site effects. Hence the resultant empirical equation for estimating spectral ratios has taken the following form:

$$R = SA_V / SA_H = C_1 + C_2 M + C_3 r_{cl} + C_4 \Gamma_1 + C_5 \Gamma_2 + P\sigma \quad (3)$$

where R is the V/H spectral ratio, M is the moment magnitude, r_{cl} is the closest horizontal distance (or Joyner-Boore distance) from the station to a site of interest in km,

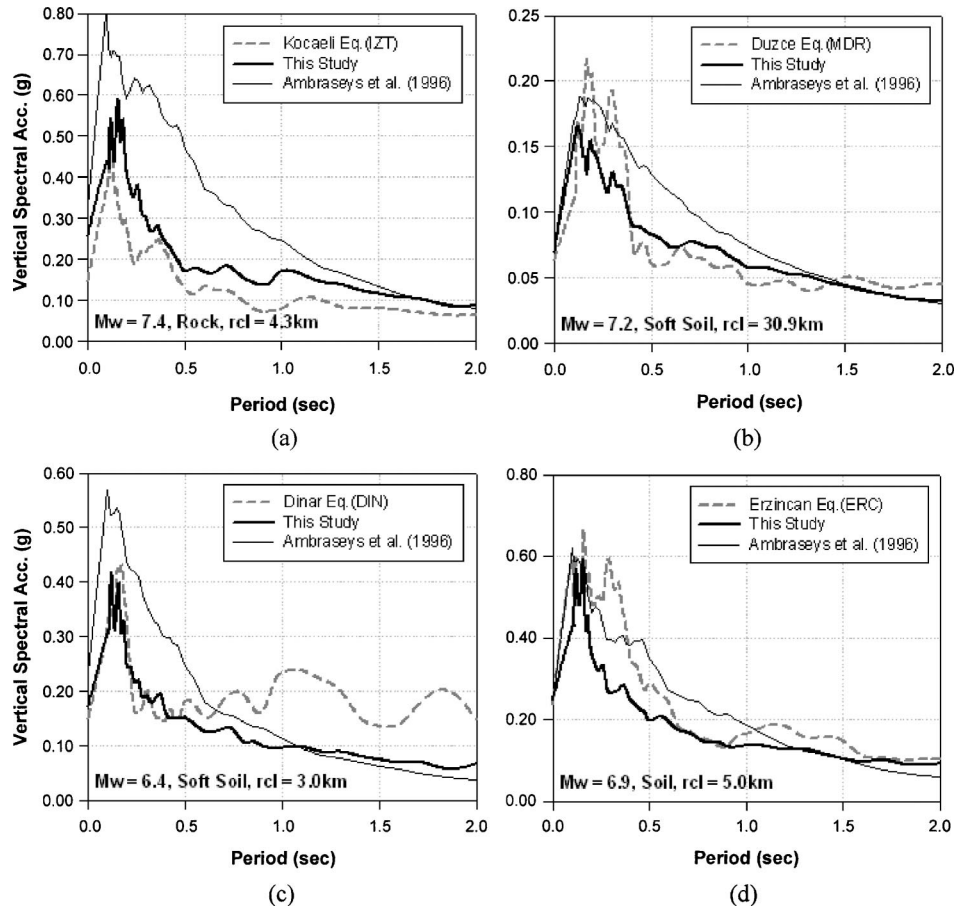


Figure 10. Comparison of mean predicted spectra from Equation 1 and Table 2 coefficients (for 5 percent of critical damping) with computed vertical response spectra of a) İzmit record (IZT), Kocaeli earthquake of 1999; b) Mudurnu record (MDR), Düzce earthquake of 1999; c) Dinar record (DIN), Dinar earthquake of 1995; and d) Erzincan record (ERC), Erzincan earthquake of 1992.

and C_1 , C_2 , and C_3 are the scaling parameters to be determined. C_4 and C_5 are soil and soft soil amplification (or de-amplification) parameters with respect to rock. Γ is an index variable controlling the local-site effects. For rock sites $\Gamma_1 = \Gamma_2 = 0$; for soil sites $\Gamma_1 = 1$ and $\Gamma_2 = 0$; for soft soil sites $\Gamma_1 = 0$ and $\Gamma_2 = 1$. The standard deviation of R is σ , and the P takes a value of 0 for mean values and 1 for 84-percentile of R . In this equation both magnitude and distance terms show geometrical attenuation, and use of logarithmic function (either log or ln) for distance term or introducing additional such terms to have anelastic meaning if the predictive model does not improve the fit.

The rational way of determining the coefficients in the median equation here is to apply a two-stage linear regression to isolate the local-site effects from magnitude and

distance dependency in a similar fashion as applied earlier. Therefore, the entire data set was regressed in the first stage disregarding the local-site effects. That yields the parameters of C_1 , C_2 , and C_3 . In the next stage, a consistent set of amplification/de-amplification parameters, C_4 and C_5 , was obtained to mimic the local-site conditions. This exercise was performed for each response period individually. The resultant coefficients for Equation 3 are presented in Table 3 with their associated standard deviation, σ . In general, coefficients of spectral ratios are consistent with each other and show minor fluctuations. The ratio of peak vertical to peak horizontal ground acceleration promises a standard deviation of 0.322, 0.268, and 0.280 for rock, soil, and soft soil sites, respectively. Generally, the estimation errors are in the admissible range when compared to those of Ambraseys et al. (1996).

The explicit investigation of V/H spectral ratios has revealed that they are strong function of period and relatively weak function of magnitude and distance, and show more dependence on magnitude than distance. The dependency of magnitude parameter is positive for up to 0.2 sec, and negative trend is observed for distance parameter up to 0.18 sec. After these spectral periods both of these trends are reversed. It is also noteworthy that the negative coefficient of magnitude in Equation 3 for spectral ratios of peak components of motion is consistent with a stronger dependence of the horizontal from that of vertical on magnitude. That is compatible with a strike-slip faulting mechanism in such a way that with increasing earthquake magnitude the horizontal acceleration increases faster than its vertical component (Ambraseys et al. 1996). The value of spectral ratio diminishes with decreasing magnitude and increasing distance at short periods. At long periods their influences are reversed. The dependence of magnitude on R is demonstrated in Figure 11. Also shown in this figure are the local-site effects. The largest short-period V/H ratios are observed to occur on soil sites at short periods where they can reach values as high as 0.9 at 0.1-sec period. The largest long-period spectral ratios are observed to occur on rock sites where they can reach values in excess of 0.5.

Comparisons of these results with those of Bozorgnia et al. (2000) are in partial agreement in that their spectral ratio at short periods can reach values at short distances in excess of 1.5 at 0.1-sec period at Holocene soil sites, and for long periods this value can reach 0.7 at rock sites. Notably, Bozorgnia et al. (2000) investigated the worldwide earthquake data recorded within 60 km of the causative fault. Ambraseys et al. (1996) reported that their spectral ratios are compatible for only near-field earthquakes ($r_{cl} < 15$ km), and for strike-slip faulting they can exceed 2 at short periods and close to 0.5 at long periods. In spite of the similarities between our results and those of Ambraseys et al. (1996) at long periods, this high discrepancy in the short period can be attributed to the characteristics of the near-field earthquakes in our data set. Nevertheless, there still exists an agreement between our results and those of Ambraseys et al. (1996) in terms of the spectral ratio of peak components of ground motion such that the ratio of peak vertical and horizontal accelerations in both studies is close to 0.7 for magnitude 7.5 earthquake at short distances, yet Ambraseys' spectral ratio diminishes more rapidly with decrease in magnitude.

In general, peak values of the vertical component of motion may exceed those of the horizontal component in the vicinity of the active faulting systems. Surprisingly, only three data points among our 19 near-field ($r_{cl} \leq 15$ km) strong motion recordings follow

Table 3. Coefficients of Equation 3 for prediction of V/H spectral ratios

Period (sec)	$R = C_1 + C_2 (M) + C_3 (r_{cl}) + C_4 \Gamma_1 + C_5 \Gamma_2 + P \sigma$					nrec*	σ_{Rock}	σ_{Soil}	$\sigma_{Soft Soil}$
	C_1	C_2	C_3	C_4	C_5				
PGA**	0.835	-0.019	-0.0007	-0.028	-0.147	100	0.322	0.268	0.280
0.100	0.632	0.033	-0.0017	0.015	-0.082	96	0.425	0.414	0.281
0.110	0.618	0.032	-0.0020	0.025	-0.028	97	0.387	0.398	0.316
0.120	0.613	0.026	-0.0018	0.000	-0.024	98	0.328	0.342	0.304
0.130	0.525	0.033	-0.0010	-0.028	-0.072	97	0.299	0.335	0.305
0.140	0.411	0.043	-0.0008	-0.033	-0.069	98	0.232	0.329	0.260
0.150	0.347	0.060	-0.0008	-0.054	-0.067	99	0.256	0.211	0.245
0.160	0.272	0.063	-0.0009	-0.026	-0.085	100	0.293	0.210	0.254
0.170	0.261	0.062	-0.0006	-0.040	-0.100	100	0.270	0.175	0.222
0.180	0.268	0.056	-0.0002	-0.014	-0.121	100	0.256	0.196	0.214
0.190	0.302	0.046	0.0000	-0.050	-0.120	100	0.256	0.191	0.214
0.200	0.353	0.035	0.0001	-0.052	-0.119	97	0.268	0.202	0.233
0.220	0.612	-0.010	0.0004	-0.035	-0.125	100	0.277	0.219	0.224
0.240	0.622	-0.010	0.0004	-0.045	-0.159	100	0.322	0.210	0.198
0.260	0.633	-0.014	0.0005	-0.030	-0.150	98	0.322	0.228	0.224
0.280	0.717	-0.031	0.0007	-0.020	-0.157	100	0.277	0.245	0.209
0.300	0.678	-0.023	0.0006	-0.010	-0.161	99	0.276	0.233	0.221
0.320	0.525	-0.004	0.0007	0.034	-0.135	98	0.215	0.265	0.224
0.340	0.487	0.001	0.0009	0.022	-0.156	98	0.214	0.323	0.219
0.360	0.383	0.006	0.0007	0.066	-0.087	99	0.266	0.303	0.233
0.380	0.438	-0.003	0.0007	0.070	-0.095	98	0.271	0.283	0.242
0.400	0.482	-0.011	0.0009	0.089	-0.110	98	0.282	0.299	0.236
0.420	0.468	-0.007	0.0008	0.088	-0.120	98	0.275	0.266	0.214
0.440	0.422	-0.001	0.0009	0.058	-0.111	98	0.266	0.214	0.214
0.460	0.420	-0.003	0.0009	0.043	-0.095	98	0.258	0.200	0.206
0.480	0.452	-0.009	0.0009	0.040	-0.085	98	0.258	0.210	0.204
0.500	0.530	-0.022	0.0010	0.036	-0.075	96	0.328	0.232	0.223
0.550	0.561	-0.024	0.0009	0.027	-0.077	98	0.273	0.228	0.242
0.600	0.643	-0.038	0.0011	0.016	-0.085	98	0.340	0.244	0.276
0.650	0.607	-0.032	0.0011	-0.020	-0.080	97	0.323	0.256	0.274
0.700	0.594	-0.028	0.0010	-0.015	-0.085	98	0.316	0.310	0.228
0.750	0.550	-0.024	0.0010	-0.040	-0.065	98	0.294	0.253	0.205
0.800	0.681	-0.047	0.0013	-0.049	-0.058	98	0.315	0.219	0.200
0.850	0.746	-0.058	0.0013	-0.041	-0.062	97	0.333	0.200	0.211
0.900	0.829	-0.071	0.0014	-0.041	-0.066	97	0.342	0.219	0.221
0.950	0.916	-0.083	0.0013	-0.022	-0.076	97	0.356	0.256	0.236
1.000	0.848	-0.063	0.0008	-0.021	-0.096	100	0.359	0.290	0.214
1.100	0.848	-0.059	0.0007	0.000	-0.120	97	0.366	0.327	0.206
1.200	0.848	-0.065	0.0008	0.018	-0.096	98	0.363	0.328	0.206
1.300	0.794	-0.054	0.0009	0.006	-0.099	97	0.313	0.315	0.179
1.400	0.836	-0.060	0.0009	0.020	-0.095	98	0.317	0.341	0.191
1.500	0.850	-0.062	0.0008	0.003	-0.090	99	0.311	0.314	0.202
1.600	0.796	-0.053	0.0008	0.001	-0.092	99	0.299	0.283	0.196
1.700	0.736	-0.042	0.0008	0.010	-0.090	99	0.306	0.310	0.219
1.800	0.721	-0.038	0.0008	0.004	-0.070	98	0.309	0.303	0.245
1.900	0.727	-0.037	0.0008	0.004	-0.076	97	0.304	0.283	0.232
2.000	0.640	-0.018	0.0004	-0.004	-0.065	99	0.315	0.290	0.255

* Number of records used for two-staged regression analysis of spectral ratios

** Coefficients for the ratio of peak vertical to peak horizontal ground acceleration

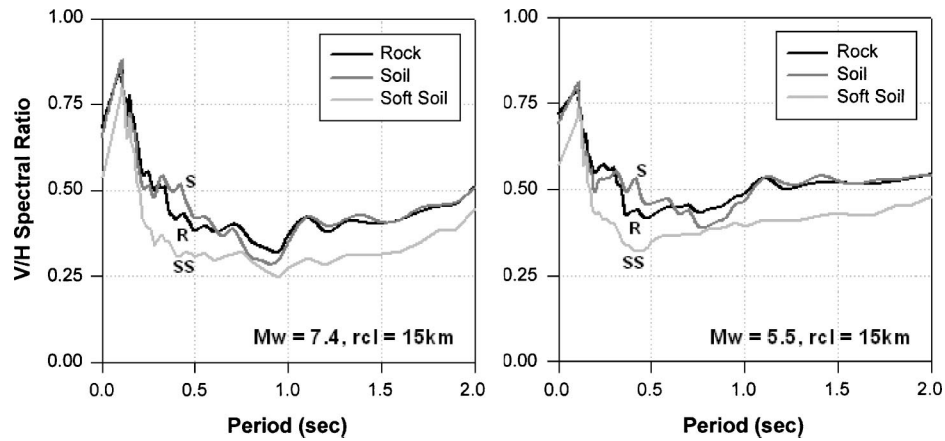


Figure 11. Peak acceleration and spectral acceleration ratios for magnitude 7.4 and 5.5 earthquakes at a closest horizontal distance of 15 km.

this general trend, and for the remaining 16 near-field records, vertical component of motion is remarkably less than that of horizontal. The distribution of spectral ratios for our near-field data set with respect to magnitude and distance is exhibited in Figure 12. Figure 13 shows the V/H spectral ratio of the near-field recordings for three different subsoil conditions. Also shown in this figure is the average of the near-field data in each site category, and our predictive curves corresponding to magnitude 6 earthquake at a distance of 10 km (taken as the average magnitude and distance based on our near-field data set). It can be clearly observed that there exists a consistency between the mean of the near-field records and predictive curves based on Equation 3. Therefore, we did not

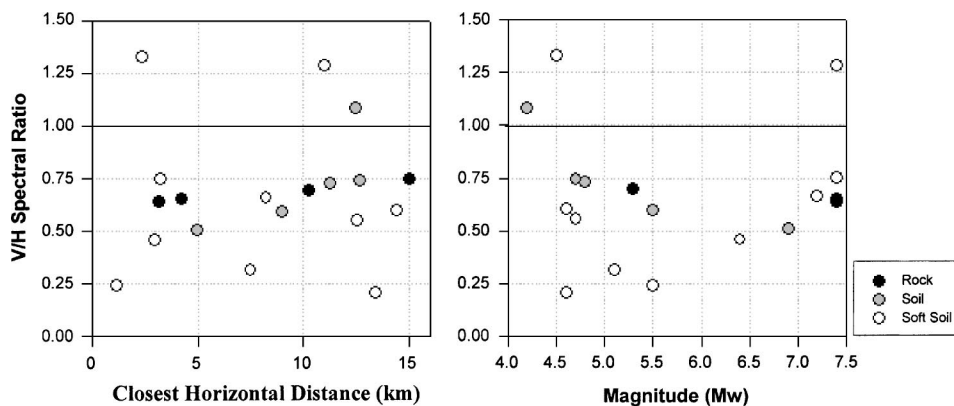


Figure 12. Distribution of the near-field data set of the ratio R of peak vertical to peak horizontal acceleration with respect to distance and magnitude.

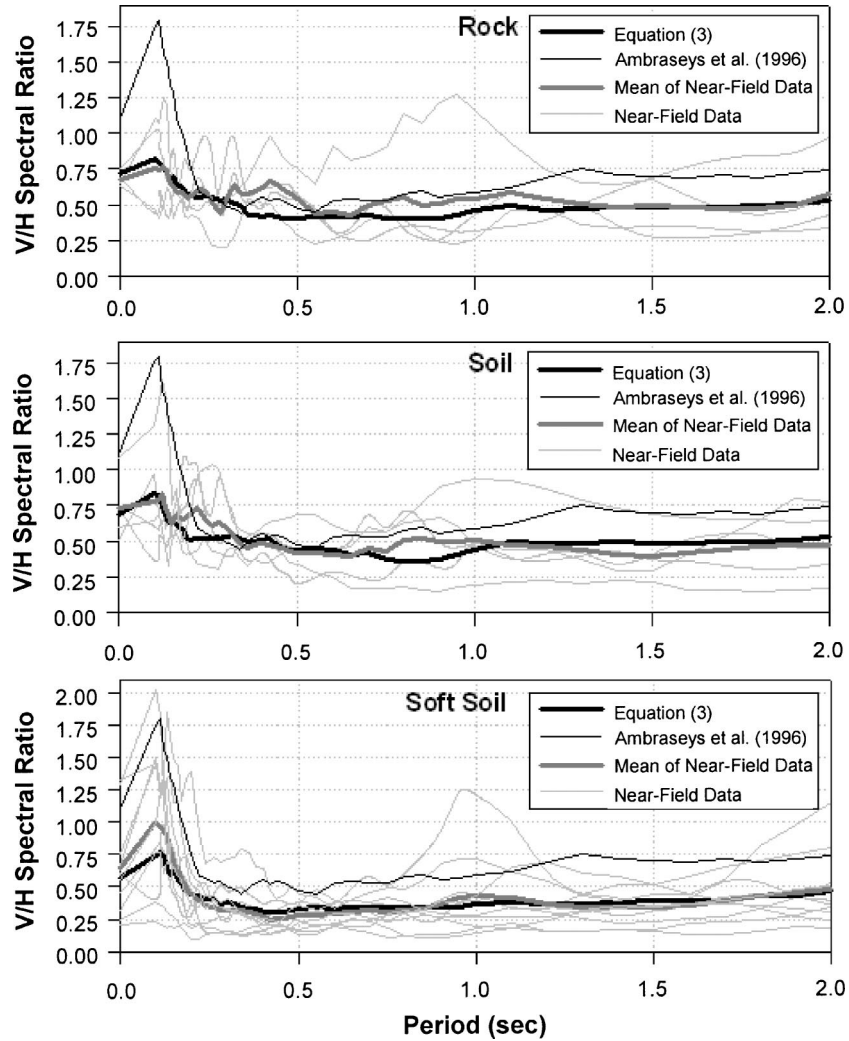


Figure 13. V/H Spectral ratio of near-field recordings in the data set for rock, soil, and soft-soil site classes; solid lines represent the results of predicted spectra and mean spectra from near-field records.

treat our near-field data separately; rather, we commingled them with the rest of the data set ($r_{cl} > 15$ km) to determine the V/H spectral ratios that can be applicable for both near-field and far-field earthquakes in Turkey.

As alluded to earlier, explicit determination of spectral ratios provided an opportunity for the cross-check of the proposed vertical and horizontal attenuation relationships. The comparisons of spectral ratio curves obtained from these two separate sources are illustrated in Figure 14 for magnitude 7.4 earthquake at 5 and 30 km of distances. Despite the discrepancies at long periods, generally there exists a good agreement between

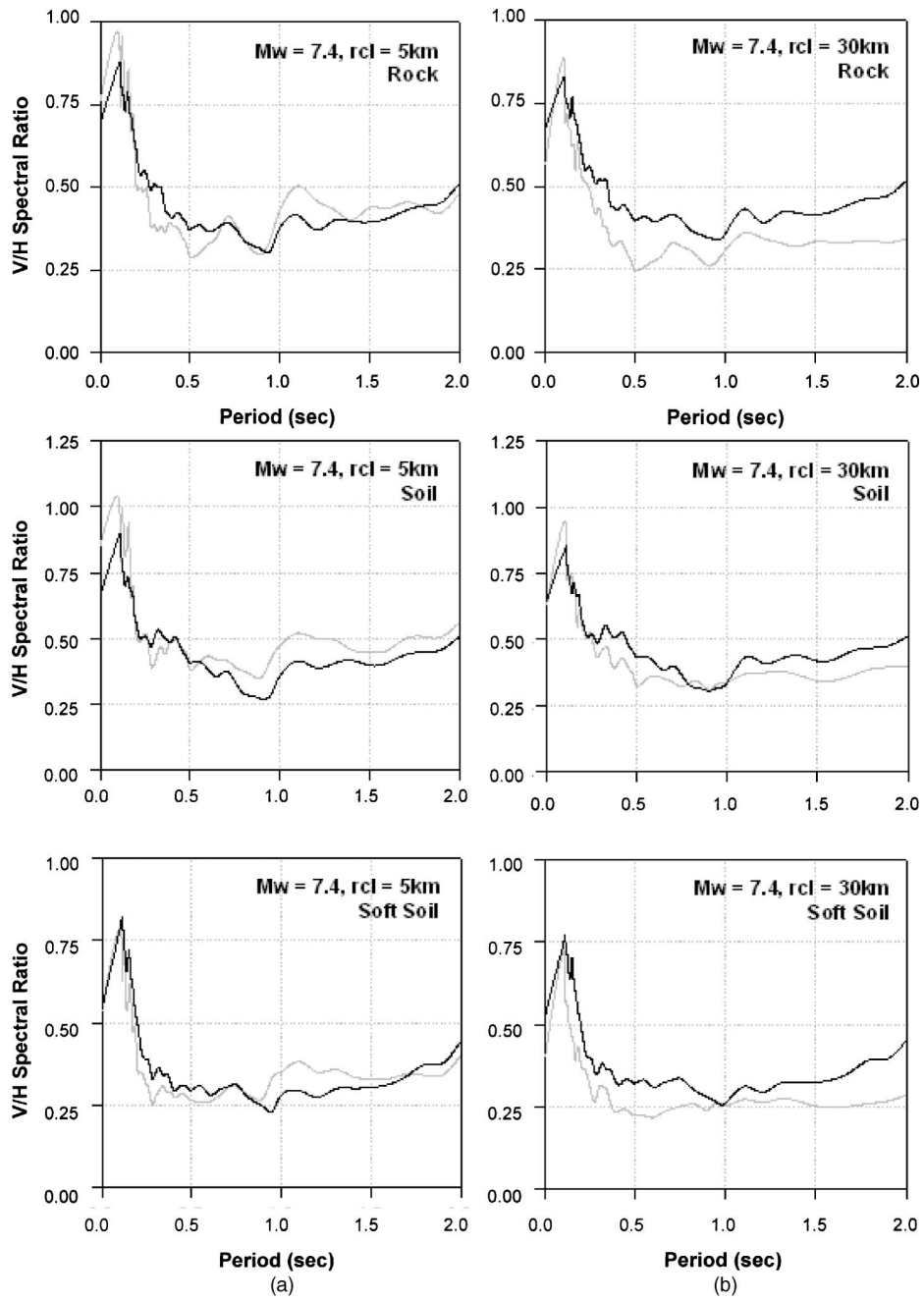


Figure 14. Comparison of V/H spectral ratios for magnitude 7.4 earthquake at a closest horizontal distance of (a) 5 km and (b) 30 km; black lines demonstrate the spectral ratios calculated based on Equation 3, gray lines correspond to the ratio of vertical to horizontal attenuation relationships.

the spectral ratios determined from Equation 3 and those explicitly obtained from predicted spectral ordinates. It is noteworthy that the horizontal attenuation model for Turkey was developed using fewer records and a different attenuation model than presented here.

UNCERTAINTY ANALYSIS

It is customary in probabilistic seismic hazard studies to distinguish the overall uncertainty of stochastic models within two orthogonal sets. The first set constitutes the aleatory and epistemic uncertainties and the second set encloses the modeling and parametric uncertainties. Aleatory uncertainty expresses the random variability of ground motions (i.e., event-to-event variations) that refers to inherent unpredictability characteristics of a future event before its occurrence, such as unique details of magnitude, propagation path, site response, and source effects. It cannot be quantified in advance, and collection of additional information may not be remedial for its reduction. However, using additional data may yield better estimates (Toro et al. 1997). Epistemic uncertainty is due to insufficient knowledge and lack of data on the precise physics of earthquake mechanism, and may be minimized by supplementary information (Kalkan and Gülkan 2004b).

Modeling uncertainty associated with the simulation procedure represents the variations between the physical process that generates the earthquake ground motions and the simplified model used for their estimation (Abrahamson et al. 1990). This type of uncertainty can be evaluated by comparing model predictions to actual observations. Since it is obtained from comparisons, the modeling uncertainty has the capability of capturing all deficiencies of the model as long as a sufficient number of events having a wide range of magnitudes and distances is provided. The other source of uncertainty in the second set is the parametric uncertainty in the values of each single parameter in the predictive model, such as model's event, path, and site-specific parameters for future earthquakes. This type of uncertainty is quantified by observing the variation in parameters inferred for several earthquakes and/or recordings (Toro et al. 1997). In practice, each of these sources of uncertainty contributes about equally to the overall uncertainty (Somerville 2000). The main difference between modeling and parametric uncertainty is the model dependency. It is also possible to reduce the overall scatter in the estimation process by including a more complex model that may require introducing more parameters, such as slip distribution, the location of hypocenter, slip and rupture velocity (Somerville 2000), and the duration and frequency content of the seismogram (Bommer and Martinez-Pereira 1999). However, this approach may not always be warranted because the attempt to increase the number of those parameters may result in an increase in the parametric uncertainty as well. It is therefore crucial to obtain the optimal variations between the modeling and parametric uncertainties.

Both modeling and parametric uncertainties consist of the prescribed aleatory and epistemic uncertainties, and that is the manifestation of significant interdependence between these two orthogonal sets. Accordingly, imperfect characteristics of our empirical models inevitably result in aleatory modeling uncertainties. On the other hand, the main source of epistemic uncertainty in our data set and predictive models is the results of the limited number of available data utilized, its quality and lack of knowledge on their

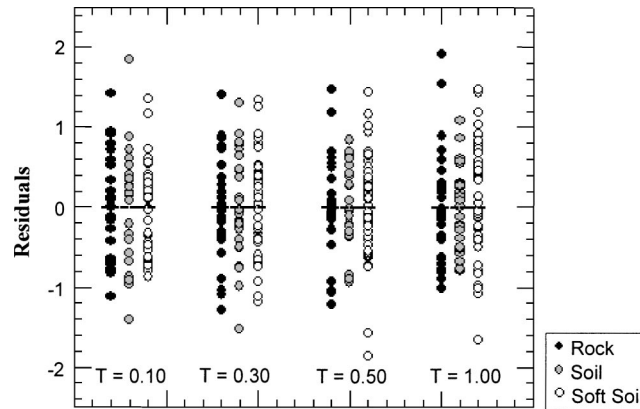


Figure 15. Distribution of residual of the natural logarithm of actual spectral amplitude with respect to estimated values from Equation 1 and Table 2 at periods of 0.1, 0.3, 0.5, and 1.0 sec for three different site categories. The horizontal bars denote mean of residuals for each site class.

sources. Our omission of aftershock data and limiting the ground motion data set with minimum vertical PGA of 10 mg caused additional epistemic parametric uncertainties. In addition to that, the lack of knowledge on geological conditions of the recording stations includes more parametric uncertainties to our predictive models.

In common practice, the uncertainties attributed to modeling can be prescribed by two goodness of fit parameters: the standard deviation and the bias, indicating on the average how close the attenuation relationship is estimating the recorded motions. In this study we did not pay attention to parametric uncertainties, and only focused on the quantification of modeling uncertainties. In view of this fact, the standard deviations of stochastic analyses given in both tabular and graphical forms are in admissible range for seismic hazard studies of Turkey when compared to other common attenuation models. Investigation of residuals showed that there is no significant bias observed in our predictions (e.g., Figures 6 and 7 for vertical PGA estimation) for each spectral period considered. That is also exemplified in the following figure (Figure 15) where the residuals of natural logarithm of the observed acceleration values produced by Equation 1 with its coefficients given in Table 2 are demonstrated for four different response periods (0.1, 0.3, 0.5, and 1.0 sec) in a similar fashion given by Ambraseys et al. (1996). The most important observation to be made from this figure may extend to range and relative distribution of residuals for each site categories. Despite the observed scatter of residuals, the mean of residuals for each site class is almost zero.

CONCLUSIONS AND RECOMMENDATIONS

The main objective of engineering seismology is to accommodate reliable estimates of expected levels of seismic ground motion as the primary input data for earthquake engineering applications. The majority of the ground motion estimation equations to serve that purpose have been developed using worldwide earthquakes. On the other

hand, significant divergence of these models from region to region accentuates the need to develop more locally concentrated predictive models. To accomplish that objective for Turkey, a consistent set of empirical equations for the estimation of vertical spectra and V/H spectral ratios was developed as the consummation of our earlier work. Based on the highlighted issues in this paper, the following conclusions and recommendations have been delineated.

The recommended attenuation relationships through Equation 1 and Table 2 are considered to be appropriate for the estimation of vertical components of PGA, and 5-percent-damped pseudo-absolute vertical acceleration response spectra for earthquakes having magnitudes in the range of (M_w) 4.5 to 7.5 at a distance of $r_{cl} < 200$ km for three different site categories (i.e., rock, soil, and soft soil). The database from which these expressions have been drawn comprises 100 sets of vertical strong-motion acceleration records obtained from 65 permanent stations. This population consisted of 33 strike-slip, 12 normal, and 2 reverse-fault mechanism earthquakes with 27 rock, 26 soil, and 47 soft-soil ground motion measurements. This data set was compiled from a variety of sources of different features and reliability, and consequently is not claimed to be pristine. It is handicapped not only because of the sheer dearth of records but also due to their poor distribution, arbitrary location, and possible interference from the response of buildings where the sensors have been stationed. We have also excluded aftershock data, and omitted records with peaks of less than about 0.01 g, and utilized broadly described site classifications due to near-total lack of knowledge of local geology at the recording stations. We did not treat the faulting mechanism as an independent parameter due to dominance of strike-slip events in our data set. Despite our efforts to double a previously compiled strong motion data library including many recent events, and performing considerable refinements and revisions, there still exists larger margins of errors in the estimates, notably for the spectral accelerations at long periods.

The study clearly manifests the influence of site geology on the vertical ground motion as it varies with respect to the horizontal. Site amplification factors are found to be less pronounceable for the vertical spectrum than those for the horizontal spectrum. The largest amplifications occur at soft-soil sites during horizontal motion, whereas, for vertical motion, soil sites yield the maximum amplification.

The spectral shape and periods at which the maxima occur are dissimilar for vertical and horizontal motions. With a faster attenuation of spectral ordinates at short periods, the shape of the vertical response spectrum shows in contrast slower decay at long periods. These differences are large enough to warrant consideration in the definition of design spectra in future editions of the regulatory Turkish Seismic Code (Regulation for Structures to be Built in Disaster Areas) (Ministry 1998).

As expected, the vertical component of motion attenuates faster than that of its horizontal with respect to the distance. The comparisons of our curves with those of other vertical attenuation relationships reveal that they overestimate our peak and spectral acceleration values at closer distances, whereas trends of our curves are generally above the others for farther distances. Among the other models we have used for comparison, the equations of Ambraseys et al. (1996) for European earthquakes yield the best match, particularly past source-to-site distance of 10 km. Whether this is caused by the fact that

APPENDIX: DATABASE OF STRONG-MOTION EVENTS IN TURKEY (AUG. 1976 –DEC. 2002)

Data No	Date (dd.mm.yy)	Event	M _w	r _d (km)	Recording Station	Data Source *	Station Coordinates	Site Soil Class	Information Source **	Peak Ground Acc. (g)		
										NS	EW	Ver.
1	19.08.1976	DENİZLİ	5.3	15.1	DNZ Denizli: Bayındırlık ve İsk. Müd.	ERD	37.8120N - 29.1140E	Soil	AMB	0.349	0.290	0.173
2	05.10.1977	ÇERKEŞ	5.4	62.1	CER Çerkeş: Meteoroloji İst.	ERD	40.8140N - 32.8830E	Soft Soil	ERD	0.036	0.039	0.016
3	16.12.1977	İZMİR	5.5	1.2	IZM İzmir: Meteoroloji İst.	ERD	38.4390N - 27.1670E	Soft Soil	TEFER	0.391	0.125	0.094
4	11.04.1979	MURADİYE	4.9	19.0	MUR Muradiye: Meteoroloji İst.	ERD	38.9900N - 43.7680E	Rock	ERD	0.046	0.045	0.025
5	28.05.1979	BUCAK	5.8	150.0	BCK Bucak: Kandilli Gözlem Evi	ERD	37.4610N - 30.5890E	Rock	ERD	0.024	0.021	0.041
6	18.07.1979	DÜRSUNBEY	5.3	10.3	DUR Dursunbey: Kandilli Gözlem İst.	ERD	39.6700N - 28.5300E	Rock	ERD	0.232	0.288	0.200
7	30.06.1981	HATAY	4.7	24.7	HTY Hatay: Bayındırlık ve İskan Müd.	ERD	36.2130N - 36.1600E	Soil	ERD	0.154	0.136	0.144
8	05.07.1983	BİGA	6.1	57.7	EDC Edincik: Kandilli Gözlem İst.	ERD	40.3600N - 27.8900E	Rock	AMB2000	0.053	0.047	0.032
9	05.07.1983	BİGA	6.1	48.7	GNN Gönen: Meteoroloji İst.	ERD	40.0800N - 27.6800E	Soft Soil	ERD	0.050	0.048	0.038
10	05.07.1983	BİGA	6.1	75.0	TKR Tekirdağ: Bayındırlık ve İsk. Müd.	ERD	40.9790N - 27.5150E	Rock	PEER, ERD	0.030	0.035	0.017
11	30.10.1983	HORASAN-NARMAN	6.5	25.0	HRS Horasan: Meteoroloji İst.	ERD	40.0430N - 42.1730E	Soft Soil	ERD	0.150	0.173	0.088
12	30.10.1983	HORASAN-NARMAN	6.5	92.5	ERZ Erzurum: Bayındırlık ve İsk. Müd.	ERD	39.9030N - 41.2620E	Soft Soil	ERD	0.035	0.025	0.032
13	29.03.1984	BALIKESİR	4.5	2.4	BLK Balıkesir: Huzur Evi	ERD	39.6500N - 27.8600E	Soft Soil	ERD	0.224	0.129	0.297
14	17.06.1984	FOÇA	5.0	98.0	FOC Foça: Gümrük Müd.	ERD	38.6400N - 26.7700E	Rock	ERD	0.024	0.023	0.024
15	12.08.1985	KİĞİ	4.9	80.8	KIG Kiğı: Meteoroloji İst.	ERD	39.3400N - 40.2800E	Soil	ERD	0.163	0.089	0.043
16	06.12.1985	KÖYCEĞİZ	4.6	14.4	KOY Köyceğiz: Meteoroloji İst.	ERD	36.9670N - 28.6808E	Soft Soil	ERD	0.103	0.114	0.069
17	05.05.1986	MALATYA	6.0	29.6	GOL Gölbaşı: Meteoroloji Müd.	ERD	37.7810N - 37.6410E	Rock	ERD	0.115	0.076	0.039
18	06.06.1986	SÜRGÜ (MALATYA)	6.0	34.7	GOL Gölbaşı: Meteoroloji Müd.	ERD	37.7810N - 37.6410E	Rock	ERD	0.069	0.034	0.018
19	06.06.1986	SÜRGÜ (MALATYA)	6.0	53.6	MLT Malatya: Bay. İsk. Müd.	ERD	38.3500N - 38.3460E	Soil	ERD	0.023	0.025	0.026
20	20.04.1988	MURADİYE	5.0	37.3	MUR Muradiye: Meteoroloji İst.	ERD	38.9900N - 43.7680E	Rock	ERD	0.050	0.051	0.021
21	12.02.1991	İSTANBUL	4.8	38.5	IST İstanbul: Kandilli Gözlem Evi	ERD	41.0800N - 29.0900E	Rock	ERD	0.026	0.018	0.010
22	13.03.1992	ERZİNCAN	6.9	5.0	ERC Erzincan: Bayındırlık ve İsk. Müd.	ERD	39.7430N - 39.5120E	Soil	ERD	0.405	0.471	0.239
23	13.03.1992	ERZİNCAN	6.9	65.0	REF Refahiye: Kaymakamlık Binası	ERD	39.9010N - 38.7690E	Soft Soil	ERD	0.067	0.086	0.032
24	06.11.1992	SIVRİHİSAR	6.1	41.0	KUS Kuşadası: Meteoroloji İst.	ERD	37.8610N - 27.2660E	Soft Soil	ERD	0.084	0.072	0.062
25	03.01.1994	İSLAHİYE	5.0	67.7	ISL İslahiye: Meteoroloji İst.	ERD	37.0500N - 36.6000E	Soil	ERD	0.021	0.019	0.019
26	24.05.1994	GİRİT	5.0	20.1	FOC Foça: Gümrük Müd.	ERD	38.6400N - 26.7700E	Rock	ERD	0.036	0.050	0.030
27	13.11.1994	KÖYCEĞİZ	5.2	17.4	KOY Köyceğiz: Meteoroloji İst.	ERD	36.9670N - 28.6880E	Soft Soil	ERD	0.073	0.097	0.058
28	29.01.1995	TERCAN	4.8	55.5	TER Tercan: Meteoroloji İst.	ERD	39.7800N - 40.3940E	Soil	ERD	0.045	0.049	0.025
29	26.02.1995	VAN	4.7	12.6	VAN Van: Bayındırlık ve İskan Müd.	ERD	38.5040N - 43.4060E	Soft Soil	ERD	0.028	0.016	0.016
30	01.10.1995	DİNAR	6.4	3.0	DIN Dinar: Meteoroloji İst.	ERD	38.0600N - 30.1550E	Soft Soil	NEI, AND	0.282	0.330	0.151
31	01.10.1995	DİNAR	6.4	39.6	CRD Çardak: Sağlık Ocağı	ERD	37.8240N - 29.6680E	Soil	AND	0.065	0.061	0.098
32	02.04.1996	KUŞADASI	4.9	55.7	KUS Kuşadası: Meteoroloji İst.	ERD	37.8610N - 27.2660E	Soft Soil	ERD	0.021	0.033	0.022
33	14.08.1996	MERZİFON	5.4	21.7	MRZ Merzifon: Meteoroloji İst.	ERD	40.8800N - 35.4590E	Soft Soil	NEI, ERD	0.033	0.102	0.029
34	21.01.1997	BULDAN	4.8	11.3	BLD Buldan: Kaymakamlık Binası	ERD	38.0450N - 28.8330E	Soil	ERD	0.039	0.024	0.028

Data No	Date (dd.mm.yy)	Event	M _w	F _a (km)	Recording Station	Data Source *	Station Coordinates	Site Soil Class	Information Source **	Peak Ground Acc. (g)		
										NS	EW	Ver.
35	22.01.1997	HATAY	5.5	9.0	HTY Hatay: Bayındırık ve İskan Müd.	ERD	36.2130N - 36.1600E	Soil	NEI, ERD	0.136	0.150	0.089
36	22.01.1997	HATAY	5.5	110.0	ISL İslahiye: Meteoroloji İst.	ERD	37.0500N - 36.6000E	Soil	ERD	0.028	0.030	0.023
37	28.02.1997	MERZİFON	4.7	26.0	MRZ Merzifon: Meteoroloji İst.	ERD	40.8800N - 35.4590E	Soft Soil	ERD	0.015	0.016	0.015
38	03.11.1997	MALAZGİRT	4.9	47.0	MLZ Malazgirt: Meteoroloji İst.	ERD	39.1700N - 42.5400E	Soft Soil	ERD	0.018	0.018	0.011
39	04.04.1998	DINAR	4.6	13.4	DIN Dinar: Meteoroloji İst.	ERD	38.0600N - 30.1550E	Soft Soil	ERD	0.135	0.131	0.028
40	04.04.1998	DINAR	4.6	48.0	CRD Çardak: Sağlık Ocağı	ERD	37.8240N - 29.6680E	Soil	ERD	0.028	0.024	0.019
41	27.06.1998	ADANA-CEYHAN	6.3	80.1	MRS Mersin: Meteoroloji İst.	ERD	36.8300N - 34.6500E	Soft Soil	NEI	0.119	0.132	0.022
42	27.06.1998	ADANA-CEYHAN	6.3	28.0	CYH Ceyhan: PTT Müd.	ERD	37.0240N - 35.8090E	Soft Soil	ERD, ADA	0.223	0.274	0.086
43	27.06.1998	ADANA-CEYHAN	6.3	95.8	ISL İslahiye: Meteoroloji İst.	ERD	37.0500N - 36.6000E	Soil	ERD	0.021	0.018	0.014
44	27.06.1998	ADANA-CEYHAN	6.3	58.8	ISK İskenderun: Meteoroloji İst.	ERD	36.6300N - 36.1500E	Soil	ERD	0.015	0.015	0.012
45	27.06.1998	ADANA-CEYHAN	6.3	89.0	HTY Hatay: Bayındırık ve İskan Müd.	ERD	36.2130N - 36.1600E	Soil	ERD	0.027	0.026	0.012
46	27.06.1998	ADANA-CEYHAN	6.3	36.0	KRT Karatas: Meteoroloji İst.	ERD	36.5610N - 35.3670E	Rock	ERD	0.029	0.033	0.020
47	09.07.1998	BORNOVA	5.1	63.0	BRN Bornova: Ziraat Fakültesi	ERD	38.4550N - 27.2290E	Soft Soil	ERD	0.027	0.013	0.006
48	17.08.1999	KOCAELİ	7.4	66.6	BRS Bursa: Sivil Sav. Müd.	ERD	40.1830N - 29.1310E	Soft Soil	ERD, PEER	0.054	0.046	0.026
49	17.08.1999	KOCAELİ	7.4	76.1	CEK Çekirgece: Nükleer Santral Bn.	ERD	40.9700N - 28.7000E	Soil	PEER	0.118	0.090	0.050
50	17.08.1999	KOCAELİ	7.4	11.0	DZC Düzce: Meteoroloji İst.	ERD	40.8440N - 31.1490E	Soft Soil	PEER, ERD	0.315	0.374	0.480
51	17.08.1999	KOCAELİ	7.4	116.0	ERG Ereğli: Kaymakamlık Bn.	ERD	40.9800N - 27.7900E	Soil	ERD	0.090	0.101	0.057
52	17.08.1999	KOCAELİ	7.4	15.0	GBZ Gebze: Tubitak Marmara Araş. Mer.	ERD	40.8200N - 29.4400E	Rock	PEER, ERD	0.265	0.141	0.198
53	17.08.1999	KOCAELİ	7.4	30.0	IZN İznik: Kaymakamlık Binası	ERD	40.4300N - 29.72 0E	Soft Soil	PEER, ERD	0.265	0.123	0.082
54	17.08.1999	KOCAELİ	7.4	49.0	IST İstanbul: Bayındırık ve İskan Müd.	ERD	41.0580N - 29.0130E	Rock	ERD	0.061	0.043	0.036
55	17.08.1999	KOCAELİ	7.4	3.2	SKR Sakarya: Bayındırık ve İskan Müd.	ERD	40.7370N - 30.3840E	Rock	PEER, ERD, AKK	0.407	N/A	0.259
56	17.08.1999	KOCAELİ	7.4	4.3	IZT İzmit: Meteoroloji İst.	ERD	40.7900N - 29.9600E	Rock	PEER, ERD, GUL	0.171	0.225	0.146
57	17.08.1999	KOCAELİ	7.4	32.0	GYN Göynük: Devlet Hastanesi	ERD	40.3960N - 30.7830E	Rock	PEER, ERD	0.138	0.118	0.130
58	17.08.1999	KOCAELİ	7.4	144.6	KUT Kutahya: Sivil Savunma Müd.	ERD	39.4190N - 29.9970E	Soil	PEER, ERD	0.050	0.060	0.023
59	17.08.1999	KOCAELİ	7.4	183.4	BLK Balıkesir: Huzur Evi	ERD	39.6500N - 27.8600E	Soft Soil	PEER, ERD	0.018	0.018	0.008
60	17.08.1999	KOCAELİ	7.4	250.0	CNK Çanakkale: Meteoroloji İst.	ERD	40.1420N - 26.4020E	Soft Soil	SUC, ERD	0.025	0.029	0.008
61	17.08.1999	KOCAELİ	7.4	67.5	ATK Ataköy	ITU	40.9890N - 28.8490E	Soft Soil	PEER	0.102	0.168	0.068
62	17.08.1999	KOCAELİ	7.4	62.3	MCD Mecidiyeköy	ITU	41.0650N - 28.9970E	Rock	PEER	0.054	0.070	0.037
63	17.08.1999	KOCAELİ	7.4	63.9	MSK Maslak	ITU	41.1040N - 29.0190E	Rock	PEER	0.054	0.038	0.031
64	17.08.1999	KOCAELİ	7.4	63.1	ZYT Zeytinburnu	ITU	40.9860N - 28.9080E	Soft Soil	PEER	0.120	0.109	0.051
65	17.08.1999	KOCAELİ	7.4	17.0	ARC Darca: Arçelik Arge Bn.	KOERI	40.8236N - 29.3607E	Soil	COS, USGS, PEER	0.211	0.134	0.083
66	17.08.1999	KOCAELİ	7.4	78.9	ATS Ambarlı: Termik Santral	KOERI	40.9809N - 28.6926E	Soft Soil	COS, USGS, PEER	0.253	0.186	0.080
67	17.08.1999	KOCAELİ	7.4	136.3	BTS M. Ereğlisi: Botaş Gas Terminali	KOERI	40.9919N - 27.9795E	Soil	COS, USGS, PEER	0.099	0.087	0.024
68	17.08.1999	KOCAELİ	7.4	69.3	DHM Yeşilköy: Havalimanı	KOERI	40.9823N - 28.8199E	Soil	COS, USGS, PEER	0.090	0.084	0.055
69	17.08.1999	KOCAELİ	7.4	3.3	YPT Yarımca: Petkim Tesistleri	KOERI	40.7639N - 29.7620E	Soft Soil	COS, USGS, AKK	0.230	0.322	0.241
70	17.08.1999	KOCAELİ	7.4	63.0	FAT Fatih: Fatih Turbesi	KOERI	41.0196N - 28.9500E	Soft Soil	COS, USGS, PEER	0.189	0.162	0.132

Data No	Date (dd.mm.yy)	Event	M _w	r _{cl} (km)	Recording Station	Data Source *	Station Coordinates	Site Soil Class	Information Source **	Peak Ground Acc. (g)		
										NS	EW	Ver.
71	17.08.1999	KOCAELİ	7.4	60.7	YKP 4. Levent: Yapı Kredi Plaza	KOERI	41.0811N - 20.0111E	Rock	COSMOS, PEER	0.041	0.036	0.027
72	17.08.1999	KOCAELİ	7.4	43.0	HAS Heybeliada: Sanatoryum	KOERI	40.8688N - 29.0875E	Rock	COSMOS	0.057	0.110	0.143
73	17.08.1999	KOCAELİ	7.4	62.7	BUR Bursa: Tofaş Fab.	KOERI	40.2605N - 29.0680E	Soft Soil	COSMOS, USGS, PEER	0.101	0.100	0.048
74	11.11.1999	SAPANCA-ADAPAZARI	5.7	17.5	SKR Sakarya: Bayındırlık ve İskan Müd.	ERD	40.7370N - 30.3840E	Rock	ERD	0.207	0.345	0.133
75	12.11.1999	DÜZCE	7.2	20.4	BOL Bolu: Bayındırlık ve İskan Müd.	ERD	40.7470N - 31.6100E	Soft Soil	PEER, ERD, AKK	0.740	0.806	0.200
76	12.11.1999	DÜZCE	7.2	8.2	DZC Düzce: Meteoroloji İst.	ERD	40.8440N - 31.1490E	Soft Soil	PEER, ERD, AKK	0.408	0.514	0.340
77	12.11.1999	DÜZCE	7.2	56.4	GYN Göynük: Devlet Hastanesi	ERD	40.3960N - 30.7830E	Rock	PEER, ERD	0.028	0.025	0.025
78	12.11.1999	DÜZCE	7.2	129.8	IZN İznik: Kaymakamlık Binası	ERD	40.4300N - 29.7200E	Soft Soil	PEER	0.022	0.021	0.010
79	12.11.1999	DÜZCE	7.2	95.0	IZT İzmit: Meteoroloji İst.	ERD	40.7900N - 29.9600E	Rock	PEER, ERD	0.022	0.024	0.022
80	12.11.1999	DÜZCE	7.2	30.9	MDR Mudurnu: Kaymakamlık Binası	ERD	40.4690N - 31.2100E	Soft Soil	ERD	0.121	0.058	0.063
81	12.11.1999	DÜZCE	7.2	169.5	KUT Kütahya: Sivil Savunma Müd.	ERD	39.4190N - 29.9970E	Soil	PEER, ERD	0.017	0.021	0.009
82	12.11.1999	DÜZCE	7.2	49.9	SKR Sakarya: Bayındırlık ve İskan Müd.	ERD	40.7370N - 30.3840E	Rock	PEER, ERD	0.017	0.025	0.018
83	12.11.1999	DÜZCE	7.2	193.3	ATS Ambarlı: Termik Santral	KOERI	40.9809N - 28.6926E	Soft Soil	COS, USGS, PEER	0.038	0.027	0.008
84	12.11.1999	DÜZCE	7.2	179.0	HAS Heybeliada: Sanatoryum	KOERI	40.8688N - 29.0875E	Rock	COS	0.024	0.028	0.016
85	12.11.1999	DÜZCE	7.2	172.5	FAT Fatih: Fatih Türbesi	KOERI	41.0196N - 28.9500E	Soft Soil	COS, USGS, PEER	0.036	0.025	0.008
86	12.11.1999	DÜZCE	7.2	101.7	YPT Yarıncı: Petkim Tesisleri	KOERI	40.7639N - 29.7620E	Soft Soil	COS, USGS, PEER	0.018	0.016	0.014
87	06.06.2000	ÇANKIRI-ORTA	6.1	30	CER Çerkeş: Meteoroloji İst.	ERD	40.8140N - 32.8830E	Soft Soil	ERD, DEM1	0.062	0.063	0.040
88	23.08.2000	HENDEK-AKYAZI	5.1	7.5	AKY Akyazı: Orman İşletme Müd.	ERD	40.6700N - 30.6220E	Soft Soil	USGS, DEM2	0.079	0.097	0.030
89	23.08.2000	HENDEK-AKYAZI	5.1	88.1	IZN İznik: Kaymakamlık Binası	ERD	40.4300N - 29.7200E	Soft Soil	USGS, DEM2	0.022	0.016	0.008
90	23.08.2000	HENDEK-AKYAZI	5.1	41.2	DZC Düzce: Meteoroloji İst.	ERD	40.8440N - 31.1490E	Soft Soil	USGS, DEM2	0.023	0.018	0.009
91	23.08.2000	HENDEK-AKYAZI	5.1	28.2	SKR Sakarya: Bayındırlık ve İskan Müd.	ERD	40.7370N - 30.3840E	Rock	USGS, DEM2	0.021	0.027	0.016
92	04.10.2000	DENİZLİ	4.7	12.7	DNZ Denizli: Bayındırlık ve İskan Müd.	ERD	37.8120N - 29.1140E	Soil	ERD	0.049	0.066	0.049
93	15.11.2000	TATVAN-VAN	5.5	200	VAN Van: Bayındırlık ve İskan Müd.	ERD	38.5040N - 43.4060E	Soft Soil	ERD	0.013	0.012	0.007
94	10.07.2001	ERZURUM-PASINLER	5.4	31.7	ERZ Erzurum: Bayındırlık ve İskan Müd.	ERD	39.9030N - 41.2620E	Soft Soil	ERD	0.020	0.022	0.027
95	26.08.2001	YİĞİLCA-DÜZCE	5.4	22.3	BOL Bolu: Bayındırlık ve İskan Müd.	ERD	40.7470N - 31.6100E	Soft Soil	ERD	0.189	0.132	0.044
96	02.12.2001	VAN	4.5	15.9	VAN Van: Bayındırlık ve İskan Müd.	ERD	38.5040N - 43.4060E	Soft Soil	ERD	0.030	0.025	0.034
97	03.02.2002	SULTANDAĞI-ÇAY	6.5	66.3	AFY Afyon: Bayındırlık ve İskan Müd.	ERD	38.7920N - 30.5610E	Soft Soil	ERD	0.114	0.094	0.036
98	03.02.2002	SULTANDAĞI-ÇAY	6.5	143	KUT Kütahya: Sivil Savunma Müd.	ERD	39.4190N - 29.9970E	Soil	GUL	0.023	0.021	0.014
99	03.04.2002	BURDUR	4.2	12.5	BRD Burdur: Bayındırlık ve İskan Müd.	ERD	37.7040N - 30.2210E	Soil	AND	0.029	0.021	0.031
100	14.12.2002	ANDIRIN-K. MARAŞ	4.8	15.95	AND Andırın: Tufan Paşa İlkokulu	ERD	37.5800N - 36.3400E	Soil	ERD	0.077	0.050	0.032

* Data source: ERD-General Directorate of Disaster Affairs, Earthquake Research Dept. (www.deprem.gov.tr); KOERI-Bogazici University, Kandilli Observatory and Earthquake Research Institute, (www.koeri.boun.edu.tr); ITU-Istanbul Technical University (www.ins.itu.edu.tr).

** Information sources: ADA-Adalier et al. (2000); AKK-Akkar et al. (2002); AMB-Ambraseys (1988); AMB2000-Ambraseys et al. (2000); ADN-Anderson et al. (2001); COS-Cosmos, (<http://db.cosmos-eq.org>); DEM 1-Demirtas et al. (2000a); DEM 2-Demirtas et al. (2000b); GUL-Gülkan et al. (2002); NEI-CNSS Catalogue, U.S. Council of National Seismic System, (<http://quake.geo.berkeley.edu/cnss/catalog-search.html>); PEER-Pacific Earthquake Engineering Research Center., (<http://peer.berkeley.edu/smcat>); SUC-Sucuoglu et al. (2001); USGS-Celebi et al. (2001).

Ambraseys' study utilized data recorded also in Turkey and/or regional resemblance between Turkey and Europe cannot be answered, except on a conjectural basis, from which we refrain.

We find that for the Turkish data set, V/H spectral ratios vary significantly with spectral periods and show relatively less dependence on local-site geology to magnitude and distance. Dependence on local-site conditions decreases at long periods. Close distances at short periods produce the largest V/H spectral ratios, where they can reach up to 0.9 at 0.1 sec at soil sites. The largest long period V/H spectral ratios are observed at 2.0 sec, where they can reach values in excess of 0.5 at rock sites. Generally, V/H ratios show more magnitude dependency than distance, and are around 0.75 at short periods, 0.4 at intermediate periods, and reach 0.5 at long periods. The ratio of vertical to horizontal PGA ranges from approximately 0.5 to 0.7 for the general comparisons. That suggests the commonly assumed value of two-thirds is reasonable for only the peak values of motion, and for the spectral periods, practicing this common value is found to be misleading in such a way that it underestimates V/H spectral ratios at short periods, but at long periods reverse is hold.

The comparisons of our empirical model of V/H spectral ratios with recently reported models show that the influence of the site geology on the amplitude of spectral ratios obtained from the model of Bozorgnia et al. (2000) are more noticeable than those distilled from our model. Notably, European model here does not consider the soil effects, as we found necessary for Turkey. In addition, there appears to be a good agreement in the amplitude of V/H ratios at long periods ($T > 0.3$ sec) when our curves are compared with Bozorgnia et al. (2000) and Ambraseys et al. (1996). At short periods this behavior is less pronounced and our curves appear to be underestimating.

In general, vertical accelerations are less than their horizontal component of strong motion data recorded. In contrast, this observation may differ for near-fault ground motions due to the significant effects of seismic source (e.g., radiation pattern, directivity, rupture model, stress drop) and also wave propagation (e.g., lateral scatterers, fault zone). Therefore, the amplitude of vertical component of ground motion may exceed that of its horizontal but falls off with distance in the close vicinity of fault tectonic area. Intriguingly, among our limited 19 near-field recordings (14 strike-slip and 5 normal faulting), the vertical component of motion exceeds that of horizontal for only a few of the recordings (Figures 12 and 13). That might be attributed to dominance of strike-slip events in our data set due to the characteristics of strike-slip fault mechanism to produce less peaks as compared to thrust and normal faults. The accumulation of additional near-field strong motion records in the future will definitely improve our understanding of the near-field seismotectonic characteristics of Turkey. Yet, if the currently observed trend is genuine, it may still suggest the nonconservatism of the two-thirds ratio at short periods, but its conservatism at long periods for near-field earthquakes as well as for far-field earthquakes.

The analysis of residuals also elucidated that the prediction of V/H spectral ratio from attenuation relationships developed independently of the horizontal and vertical

components of PGA and spectral accelerations are unbiased. That advocates the applicability of the proposed empirical model via Equation 3 with the coefficients in Table 3 to estimate the V/H spectral ratios for Turkey.

It is a truism that as additional strong motion records, shear wave velocity profiles for the recording sites, and better determined distance data become available for Turkey, the attenuation relationships derived in this study can be progressively refined, and their uncertainties can be reduced.

ACKNOWLEDGMENTS

Sincere thanks are extended to Dr. Mehmet Çelebi at USGS, Ulubey Çeken, Zahide Çolakoğlu and Tülay Uğraş at the Earthquake Research Department (ERD) of General Directorate of Disaster Affairs, and Tolga Yılmaz at Earthquake Research Center of Middle East Technical University for their support. Most of our data has been supplied originally by ERD. Boğaziçi University's Kandilli Observatory (KOERI), and Istanbul Technical University (ITU) data have also been used in this work.

REFERENCES

- Abrahamson, N. A., and Litehiser, J. J., 1989. Attenuation of vertical peak accelerations, *Bull. Seismol. Soc. Am.* **79**, 549–580.
- Abrahamson, N. A., Somerville, P. G., and Cornell, C. A., 1990. Uncertainty in numerical strong motion predictions, *Proc. 4th U.S. National Conference on Earthquake Engineering*, **1**, pp. 407–416.
- Adalier, K., and Aydingun, O., 2000. Geotechnical issues of the June 27, 1998 Adana-Ceyhan earthquake, *Proc. 12th World Conference on Earthquake Engineering*, Paper No. 0653.
- Akkar, S., and Gülkan, P., 2002. A critical examination of near-field accelerograms from the sea of Marmara region earthquakes, *Bull. Seismol. Soc. Am.* **92** (1), 428–447.
- Ambraseys, N. N., 1988. Engineering seismology, *Earthquake Eng. Struct. Dyn.* **17**, 1–105.
- Ambraseys, N. N., and Simpson, K. A., 1996. Prediction of vertical response spectra in Europe, *Earthquake Eng. Struct. Dyn.* **25** (4), 401–412.
- Ambraseys, N. N., and Jackson, J. A., 2000. Seismicity of the sea of Marmara (Turkey) since 1500, *Geophys. J. Int.* **141**, F1–F6.
- Anderson, J. G., Sucuoglu, H., Erberik, A., Yılmaz, T., Durukal, E., Erdik, M., Anooshehpour, R., Brune, J. N., and Shean-Der, N., 2000. Earthquake of August 17, 1999: Reconnaissance report, chapter 6-implications for seismic hazard analysis, *Earthquake Spectra* **16**, 113–137.
- Anderson, J. G., Zeng, Y., and Sucuoglu, H., 2001. Analysis of accelerations from the 1 October 1995 Dinar, Turkey earthquake, *Bull. Seismol. Soc. Am.* **91** (6), 1433–1455.
- Atkinson, G. M., and Boore, D. M., 1997. Some comparisons between recent ground motion relations, *Seismol. Res. Lett.* **68** (1), 24–40.
- Bommer, J. J., and Martinez-Pereira, A., 1999. The effective duration of earthquake strong motion, *J. Earthquake Eng.* **3**, 127–172.
- Boore, D. M., Joyner, W. B., and Fumal, T. E., 1993. Estimation of response spectra and peak accelerations from western North American earthquakes: An interim report, *U.S. Geol. Surv. Open-File Report 93-509*, Menlo Park, CA.
- Boore, D. M., Joyner, W. B., and Fumal, T. E., 1997. Equations for estimating horizontal re-

- response spectra and peak acceleration from Western North American earthquakes: A summary of recent work, *Seismol. Res. Lett.* **68** (1), 128–153.
- Bozorgnia, Y., Campbell, K. W., and Niazi, M., 2000. Observed spectral characteristics of vertical ground motion recorded during worldwide earthquakes from 1957 to 1995, *Proc. 12th World Conference on Earthquake Engineering*, Paper No. 2671.
- California Institute of Technology (Caltech), 1972. Analyses of strong motion earthquake accelerograms-response spectra. Vol. III, Part A, *Report No. EERL 72-70*, Earthquake Engineering Research Laboratory, Pasadena, CA.
- Campbell, K. W., 1985. Strong motion attenuation relations: A ten-year perspective, *Earthquake Spectra* **1** (4), 759–803.
- Campbell, K. W., 1997. Empirical near source attenuation relationships for horizontal and vertical components of peak ground acceleration, peak ground velocity, and pseudo-absolute acceleration response spectra, *Seismol. Res. Lett.* **68** (1), 154–179.
- Çelebi, M., Akkar, S., Gulerce, U., Sanli, A., Bundock, H., and Salkin, A., 2001. Main shock and aftershock records of the 1999 Izmit and Düzce, Turkey earthquakes, *U.S. Geol. Surv. Open-File Report 01-163*, Menlo Park, CA.
- Demirtas, R., Erkmén, C., and Yaman, M., 2000a. Preliminary Report of the Orta, Cankiri Earthquake of June 06 2000 (in Turkish), 2000, General Directorate of Disaster Affairs, Earthquake Research Department (ERD), Ankara, Turkey.
- Demirtas, R., Erkmén, C., and Yaman, M., 2000b. August 23rd, 2000 Karadere, Hendek-Akyazi Earthquake Report (in Turkish), 2000. General Directorate of Disaster Affairs, Earthquake Research Department (ERD), Ankara, Turkey.
- Gülkan, P., and Kalkan, E., 2002. Attenuation modeling of recent earthquakes in Turkey, *J. Seismol.* **6**, 397–409.
- Gülkan, P., Özcebe, G., and Sucuoğlu, H., 2002. *February 3rd Sultandagi-Cay Earthquake Engineering Report*, Earthquake Eng. Res. Cent., Middle East Tech. Univ., Ankara, Turkey.
- Hanks, T., and Kanamori, H., 1979. A moment magnitude scale, *J. Geophys. Res.* **84** (2), 348–350.
- Kalkan, E., and Gülkan, P., 2004a. Site dependent spectra derived from ground motion records in Turkey, *Earthquake Spectra*, to be published in issue **20** (4).
- Kalkan, E., and Gülkan, P., 2004b. Estimation of uncertainties and parametric sensitivity in peak ground attenuation equation using Monte Carlo simulation, *J. Seismol.* (submitted for publication).
- Kramer, S. L., 1996. *Geotechnical Earthquake Engineering*, Prentice Hall.
- Ministry of Public Works and Settlement, 1998. *Regulation for Structures to Be Built in Disaster Areas*, Ankara, Turkey.
- Newmark, N. M. and Hall, W. J., 1982. *Earthquake Spectra and Design*, Earthquake Engineering Research Institute, Berkeley, CA.
- Parsons, T., Toda, S., Stein, R. S., Barka, A., and Dieterich, J. H., 2000. Heightened odds of large earthquakes near Istanbul: An interaction-based probability calculation, *Science* **288**, 661–665.
- Rathje, E., Idriss, I. M., Somerville, P., Ansal, A., Bachhuber, J., Baturay, M., Frost, D., Lettis, W., Sozer, B., and Ugras, T., 2000. Kocaeli, Turkey, earthquake of August 17, 1999: Reconnaissance report, chapter 4-strong ground motions and site effects, *Earthquake Spectra* **16**, 65–96.
- Safak, E., Erdik, M., Beyen, K., Carver, D., Cranswick, E., Çelebi, M., Durukal, E., Ellsworth,

- W., Holzer, T., Meremonte, M., Mueller, C., Ozel, O., and Toprak, S., 2000. Kocaeli, Turkey, earthquake of August 17, 1999: Reconnaissance report, chap. 5—Recorded Mainshock and Aftershock Motions, *Earthquake Spectra* **16**, 97–112.
- Somerville, P., 2000. Reducing uncertainty in strong motion predictions, *Proc. 12th World Conference on Earthquake Engineering*, Paper No. 2688.
- Spudich, P., Joyner, W. B., Lindh, A. G., Boore, D. M., Margaris, B. M., and Fletcher, J. B., 1999. SEA99: A revised ground motion prediction relation for use in extensional tectonic regimes, *Bull. Seismol. Soc. Am.* **89** (5), 1156–1170.
- Sucuoglu, H., Gülkan, P., Yilmaz, C., Bakir, S., Özcebe, G., Ersoy, U., Tankut, T., Gür, T., Akkar, S., Erberik, A., and Yilmaz, T., 2001. *Marmara and Düzce Earthquakes Engineering Report* (in Turkish), Earthquake Eng. Res. Cent., Middle East Tech. Univ., Ankara, Turkey.
- Toro, G. R., Abrahamson, N. A., and Scheinder, J. F., 1997. Model of strong ground motions from earthquakes in Central and Eastern North America: Best estimates and uncertainties, *Seismol. Res. Lett.* **68** (1), 41–57.
- Wells, D. L., and Coppersmith, K. J., 1994. New empirical formula among magnitude, rupture length, rupture width, rupture area, and surface displacement, *Bull. Seismol. Soc. Am.* **84** (4), 974–1002.

(Received 17 July 2003; accepted 2 February 2004)